Available online at www.sciencedirect.com

ScienceDirect

MATTER AND RADIATION AT EXTREMES

Matter and Radiation at Extremes 2 (2017) 225–242

www.journals.elsevier.com/matter-and-radiation-at-extremes

Review Article

Electron-positron pair production in ultrastrong laser fields

Bai Song Xie [a,b,*], Zi Liang Li [a,c], Suo Tang [a,d]

[a] College of Nuclear Science and Technology, Beijing Normal University, Beijing 100875, China
[b] Beijing Radiation Center, Beijing 100875, China
[c] School of Science, China University of Mining and Technology, Beijing 100083, China
[d] Max-Planck-Institut für Kernphysik, Saupfercheckweg 1, 69117 Heidelberg, Germany

Received 24 February 2017; revised 19 May 2017; accepted 10 July 2017
Available online 29 July 2017

Abstract

Electron–positron pair production due to the decay of vacuum in ultrastrong laser fields is an interesting topic which is revived recently because of the rapid development of current laser technology. The theoretical and numerical research progress of this challenging topic is reviewed. Many new findings are presented by different approaches such as the worldline instantons, the *S*-matrix theory, the kinetic method by solving the quantum Vlasov equation or/and the real-time Dirac–Heisenberg–Wigner formalism, the computational quantum field theory by solving the Dirac equation and so on. In particular, the effects of electric field polarizations on pair production are unveiled with different patterns of created momentum spectra. The effects of polarizations on the number density of created particles and the nonperturbative signatures of multiphoton process are also presented. The competitive interplay between the multiphoton process and nonperturbation process plays a key role in these new findings. These newly discovered phenomena are valuable to deepen the understanding of pair production in complex fields and even have an implication to the study of strong-field ionization. More recent studies on the pair production in complex fields as well as beyond laser fields are briefly presented in the view point of perspective future.

PACS Codes: 12.20.Ds; 11.15.Tk; 32.80.-t

Keywords: Strong field physics; Vacuum pair production; Nonlinear quantum electrodynamics

1. Introduction

In 1928, Dirac proposed the positron existence physically to explain the negative energy solution of Dirac equation [1] and a few years later in 1933, Anderson confirmed it experimentally [2]. Since then the electron–positron (e^+e^-) pair production from vacuum in the presence of a strong field became one of the well-known predictions of quantum electrodynamics (QED) [3–5]. In particular, it is an important testing field to probe the quantum vacuum structure, since the vacuum is full of virtual particles and fluctuations, then it is natural to regard it as a special polarized medium which induces nonlinear effects on Maxwell equations. Indeed in 1936, Heisenberg and Euler had recognized this point firstly and derived the modified effective Lagrangian action [4] for a static electromagnetic field. They also claimed that the vacuum decay probability could be obtained by summing an infinite number of poles in the one-loop effective Lagrangian action. The more direct calculation of the vacuum decay probability was given by Schwinger using the proper-time method in 1951 [5]. He obtained the pair production rate for the constant electric field E. According to Schwinger's formula, the pair production rate, $\Gamma \sim \exp(-\pi E_{cr}/E)$, is exponentially suppressed for a weak field, where $E_{cr} = m^2c^3/$

* Corresponding author. College of Nuclear Science and Technology, Beijing Normal University, Beijing 100875, China.
E-mail address: bsxie@bnu.edu.cn (B.S. Xie).
Peer review under responsibility of Science and Technology Information Center, China Academy of Engineering Physics.

http://dx.doi.org/10.1016/j.mre.2017.07.002

$e\hbar \approx 1.32 \times 10^{16}$ V/cm is the critical field strength. In the expression of E_{cr}, m and $-e$ are the electron mass and charge respectively, $\hbar$ is the Planck constant and c is the speed of light in vacuum. Note that sometimes the simple expression of $E_{cr} = m^2/e$ is also used when the natural units $h = c = 1$ are employed. Obviously the corresponding laser intensity I_{cr} is about 10^{29} W/cm^2 so that it is still a rather difficult task for experimental detection of vacuum pair creation because current laser intensity is much lower than I_{cr}. In addition to the constant electric field, Sauter-type electric field is another type of external field which can give an analytical result of pair creation. This field had been studied in detail by Narozhnyi and Nikishov [6] and Popov [7] in 1970s. In 1970, Brezin and Itzykson [8] extended the research to the pair production from vacuum in a time-dependent sinusoidal electric field and found the multiphoton pair production process which was different from the Schwinger tunneling process.

On the other hand, as the rapid development of laser technology, especially the chirped pulse amplification, the laser intensity has been improved greatly [9,10], for example, the laser intensity has reached about 10^{22} W/cm^2 [11]. More exciting achievement is the high-intensity and ultrashort laser facilities under construction, such as the Extreme Light Infrastructure (ELI) [12], the Exawatt Center for Extreme Light Studies (XCELS) [13], and the High Power Laser Energy Research (HiPER) [14], in which the intensity is expected to be 10^{25}– 10^{26} W/cm^2 and the field is beyond the relativistic regime of 10^{18} W/cm^2. This ultrastrong laser field is very helpful to clarify the radiation reaction in classical electrodynamics as well as QED [15–18] and also to probe the structure of quantum vacuum [19–21]. Moreover, the X-ray free electron laser (XFEL) [22,23], may provide a subcritical electric field which can produce a considerable number of e^+e^- pairs [24,25]. Therefore, these technology advances stimulate researchers' renewed interests to explore significant phenomena of e^+e^- pair production by various different methods in present and expected future ultrastrong laser fields, see the recent review article [26]. These research methods include the worldline instantons technique [27–32], the S-matrix method [33–38], the semiclassical approach such as the Wentzel–Kramers–Brillouin (WKB) approximation [39–43], the kinetic method such as the quantum Vlasov equation (QVE) [24,25,44–49] and the real-time Dirac–Heisenberg–Wigner (DHW) formalism [50–52], the computational quantum field theory (CQFT) such as by solving the Dirac equation [53–60] numerically, and the real-time lattice gauge theory or/and classical-statistical field theory approach which can self-consistently account for the back reaction of created particles on the background field [61–64].

Based on the statement mentioned above, there are two different pair production processes or/and mechanisms. One is the tunneling mechanism, which is sometimes also called as the Schwinger mechanism [5,31], and the other is the multiphoton mechanism [8,65,66]. Obviously these processes or/and mechanisms have been recognized extensively in atomic strong field ionization (SFI) problem for many years [67–71]. Therefore similarly the well known Keldysh parameter $\gamma = m\omega/eE$ [67], where ω is the frequency of field, can also be used to characterize the pair production and distinguish these two processes. In general, $\gamma \ll 1$ corresponds to the pair creation process in a low frequency and strong field, i.e., the Schwinger mechanism, and $\gamma \gg 1$ corresponds to the pair production in a high frequency and weak field, i.e., the multiphoton process [8]. However, there is a great challenge when $\gamma \sim 1$ because there exists an interplay and competition effect between these two mechanisms on studied problems.

In the experimental aspect for the pair production, the pair production was first observed as early as about 20 years ago, in 1997, at Stanford Linear Accelerator Center (SLAC) as an E-144 experiment performance. It was realized through a collision of a 46.6 GeV electrons beam with a laser beam of 1.3×10^{18} W/cm^2 [65,66,72]. The high energy γ photon was first produced via nonlinear Compton scattering of electron beams with laser, and then the e^+e^- pairs were created via the multiphoton Breit-Wheeler process ($\omega + n\omega_0 \rightarrow e^+ + e^-$) by the created high energy γ photon colliding with the coming laser. The theoretical studies on the possibility of observing the Schwinger-pair-creation mechanism in heavy-ion collisions have been considered many years ago, however, the experimental observation has not led to its verification. For details, readers can refer to the review article of Ref. [73].

In this review paper, we focus on the theoretical and numerical research on the pair production. While introducing some important results and advances of this topic with different methods like worldline instantons, S-matrix, WKB, QVE and DHW as well as CQFT, we mainly present some works which have been done recently by the research group in Beijing Normal University [32,38,42,46–48,51,52,60]. Particularly, the effects of electric field polarization on pair production are unveiled with different patterns of created momentum spectra. Meanwhile the interplay between the multiphoton process and nonperturbation process plays a key role on some new findings, i.e., the multiple-slit interference effect, the ring structure of created momentum spectra, the node existence and disappearance in momentum spectra depending on the polarization and so on. These distinguishable momentum signatures in nonperturbative multiphoton pair production could be relevant for providing the output information of created particles, for example, the momentum signatures associated with the node positions could be used to distinguish the orbital angular momentum (OAM) of created pairs, and they can reveal the input information of ultrashort laser pulses.

It should be emphasized that the study of pair production from vacuum in ultrastrong laser fields is not only important theoretically but also expected to be helpful to expand the technology applications for matter and radiation at extreme conditions in the future. In the final part of this review paper, we also give an interesting outlook and perspective on pair production as an interesting and challenging physics problem.

2. Pair production studied by worldline instantons

Feynman [74] proposed the path integral method originally which becomes a powerful theoretical analysis tool as well as

a computational approach in many processes of QED [75], in particular for the studies on perturbation and nonperturbative phenomena. This is now called the worldline instanton technique and has also been extended to study e^+e^- pair production in an external field in terms of the imaginary part of the effective Lagrangian, as the imaginary part is associated with the famous Schwinger's formula [5] under a constant field. In fact as early as in the beginning of 1980s, Affleck et al. [27] had studied the pair production in a constant field in scalar QED by applying instanton technique to Feynman worldline path integral. Kim and Page [28] proposed that the single instanton and multi-instantons of quantum tunneling may be related with the single pair and multipair production. Dunne and Schubert [29] studied in detail the pair production in both spatial and temporal inhomogenous fields. In particular, they computed the imaginary part of the one-loop effective action in scalar QED for a wide class of inhomogeneous background electric fields. Dunne and Wang [30] also extended the worldline instanton technique to compute the vacuum pair production rate for spatially inhomogeneous background electric fields, with the spatial inhomogeneity being genuinely two or three dimensions, for both the magnitude and direction of the electric field. We also calculated the e^+e^- pair production rate for a time-dependent elliptic polarization field in 2012 [32]. As an illustration we just give a simple introduction about the worldline instantons technique and the application to the study of pair production in linear and circular polarized fields.

As shown in Refs. [27,29], the worldline action S_0

$$S_0 = m\sqrt{\int_0^1 \mathrm{d}u\dot{x}^2} + \mathrm{i}e\int_0^1 \mathrm{d}uA\cdot\dot{x} \tag{1}$$

is stationary if the path $x_\mu(u)$ satisfies

$$m\frac{\ddot{x}_\mu}{\sqrt{\int_0^1 \mathrm{d}u\dot{x}^2}} = \mathrm{i}eF_{\mu\nu}\dot{x}_\nu, \tag{2}$$

where $x_\mu(u)$ as a periodic solution of Eq. (2) is called a worldline instanton. Obviously the stationary instanton paths should satisfy a conservation law of $\dot{x}^2 \equiv a^2 =$ constant with the constant $a \gg 1/m$, which meets a weak-field condition comparable to the Schwinger critical field.

Usually the pair production rate is associated with the imaginary part of the effective action $\Gamma(A)$ which has an exponental form of S_0 as

$$\mathrm{Im}\Gamma(A) \sim \mathrm{e}^{-S_0}. \tag{3}$$

We emphasize that the effective action contributes a leading part of the pair production rate but the subleading prefactor contribution seems to be difficult to get. Therefore many works are only attributed to the leading exponential term, i.e. S_0.

Usually by a Wick rotation as $x_4 = \mathrm{i}t$ and assuming the four-vector potential for a spatially homogeneous and time-dependent field as $A = (A_1(x_4), A_2(x_4),0,0)$, the field strengths are $F_{14} = -F_{41} = -A_1'(x_4)$ and $F_{24} = -F_{42} = -A_2'(x_4)$. Therefore we have the following motion equations

$$\dot{x}_1 = -\frac{\mathrm{i}ea}{m}A_1(x_4), \tag{4}$$

$$\dot{x}_2 = -\frac{\mathrm{i}ea}{m}A_2(x_4), \tag{5}$$

and $\dot{x}_1^2 + \dot{x}_2^2 + \dot{x}_4^2 = a^2$. Further we get

$$\left|\dot{x}_4\right| = a\sqrt{1 + \left[\frac{eA_1(x_4)}{m}\right]^2 + \left[\frac{eA_2(x_4)}{m}\right]^2}. \tag{6}$$

And now it is ready to get the worldline action in the stationary conditions as

$$S_0 = ma + \mathrm{i}e\int_0^1 \mathrm{d}u(A_1\cdot\dot{x}_1 + A_2\cdot\dot{x}_2) \tag{7}$$

$$= \frac{m}{a}\int_0^1 \mathrm{d}u(\dot{x}_4)^2. \tag{8}$$

In the following, we discuss two cases of linear and circular polarized fields with sinusoidal temporal profile. First it is known that for the linear polarization case [29], the stationary action S_0 is given by

$$S_0 = \frac{m}{a}\int_0^1 \mathrm{d}u(\dot{x}_4)^2 \tag{9}$$

$$= \frac{nm^2}{eE}\frac{4\sqrt{1+\gamma^2}}{\gamma^2}[\boldsymbol{K}(k_1) - \boldsymbol{E}(k_1)], \tag{10}$$

where $\boldsymbol{K}$ and $\boldsymbol{E}$ are the complete elliptic integrals of the first and second kind, respectively, with $k_1^2 = \gamma^2/(1+\gamma^2)$. In some publications, e.g., Refs. [8,22], a convenient function is introduced as

$$g(\gamma) \equiv \frac{4}{\pi}\int_0^1 \mathrm{d}u\left(\frac{1-u^2}{1+\gamma^2u^2}\right)^{1/2} \tag{11}$$

$$= \frac{4}{\pi}\frac{\sqrt{1+\gamma^2}}{\gamma^2}[\boldsymbol{K}(k_1) - \boldsymbol{E}(k_1)]. \tag{12}$$

Thus the stationary action S_0 is simplified as

$$S_0 = \frac{n\pi m^2}{eE}g(\gamma) \tag{13}$$

with $g(\gamma)$ in two limiting cases as

$$g(\gamma)=\begin{cases} 1-\dfrac{1}{8}\gamma^2+\mathcal{O}(\gamma^4), & \gamma\ll 1,\\ \dfrac{4}{\pi\gamma}\ln(4\gamma)+\mathcal{O}(1/\gamma), & \gamma\gg 1. \end{cases} \tag{14}$$

From these two limiting cases we can get the following familiar results: (i) For a low frequency and strong field which corresponds to $\gamma \ll 1$, one can get $S_0 \sim n\pi\frac{E_{cr}}{E}\left(1-\frac{\gamma^2}{8}\right)$. Pair production is dominated by the Schwinger mechanism corresponding to nonperturbative processes of vacuum decay interacted by the background field; (ii) For a high frequency and weak field which corresponds to $\gamma \gg 1$, one can get the pair production rate $\Gamma \sim e^{-S_0} \sim \left(\frac{eE}{m\omega}\right)^{\frac{4nm}{\omega}}$. Pair production is dominated by the multiphoton mechanism corresponding to perturbative processes of vacuum decay interacted by the background field. Obviously these results appeared in many publications [5,8,22,29,76] have now been known as the classical samples as an application of worldline instanton technique successfully.

On the other hand, for the circular polarization case, we have two equations to determine τ_0 and s by

$$\int_0^{\tau_0}\frac{s-\cosh\tau}{\sqrt{\gamma^2+(s-\cosh\tau)^2-\sinh^2\tau}}\mathrm{d}\tau=0, \tag{15}$$

and

$$\gamma^2+(s-\cosh\tau_0)^2-\sinh^2\tau_0=0. \tag{16}$$

It should be pointed out that Eq. (15) exhibits the condition of periodic motion character of instanton, refer to Ref. [39], where parameter s is associated with the integral constant in the expression of A_2 (x_4) by Eq. (5), and Eq. (16) is the stationary condition to determine the turning point τ_0. At first we write

$$\mathrm{d}u=\frac{\gamma}{a}\frac{\mathrm{d}x_4}{\sqrt{\gamma^2+(s-\cosh\tau)^2-\sinh^2\tau}},$$

and then by using the relation of Eq. (16) one obtains a convenient expression

$$\mathrm{d}u=\frac{\gamma}{a}\frac{\mathrm{d}x_4}{\sqrt{2s(\cosh\tau_0-\cosh\tau)}},$$

which has the solution

$$x_4=\frac{2}{\omega}\sinh^{-1}\left[\sinh(\tau_0/2)\mathrm{sd}\left(\frac{\sqrt{s}\cosh(\tau_0/2)}{\gamma}\omega a u,k_2\right)\right]$$

where $k_2=\tanh(\tau_0/2)$. Here $\mathrm{sd}(u,k)=\mathrm{sn}(u,k)/\mathrm{dn}(u,k)$ is the sine-to-delta amplitude Jacobi elliptic function and $0\le k\le 1$ is the real elliptic parameter. In order to evaluate the stationary action S_0 we need the expression of $\dot{x_4}(u)$.

$$\dot{x_4}=2a\frac{\sqrt{s}}{\gamma}\sinh(\tau_0/2)\mathrm{cd}[4n\boldsymbol{K}(k_2)u,k_2)]. \tag{17}$$

Here $\mathrm{cd}(u,k)=\mathrm{cn}(u,k)/\mathrm{dn}(u,k)$ is the cosine-to-delta amplitude Jacobi elliptic function and $0\le k\le 1$ is the real elliptic parameter. The constant a can be determined by the periodic condition as

$$a=\frac{\gamma}{\omega\sqrt{s}\cosh(\tau_0/2)}4\boldsymbol{K}(k_2)n,$$

where n here is a positive integer. Thus the stationary action S_0 is now becoming

$$S_0=\frac{m}{a}\int_0^1\mathrm{d}u(\dot{x_4})^2 \tag{18}$$

$$=\frac{nm^2}{eE}\frac{16\sqrt{s}\cosh(\tau_0/2)}{\gamma^2}[\boldsymbol{K}(k_2)-\boldsymbol{E}(k_2)]. \tag{19}$$

Also a convenient expression as $S_0=\frac{n\pi m^2}{eE}g(\gamma)$ can be got if a function of $g(\gamma)$ is introduced as

$$\begin{aligned} g(\gamma)&=\frac{16\sqrt{s}\cosh(\tau_0/2)}{\pi\gamma^2}[\boldsymbol{K}(k_2)-\boldsymbol{E}(k_2)]\\ &\equiv\frac{16\sqrt{s}\sinh^2(\tau_0/2)}{\pi\gamma^2}\int_0^1\mathrm{d}u\sqrt{\frac{1-u^2}{1+\sinh^2(\tau_0/2)u^2}}. \end{aligned}$$

It is noted that the function of $g(\gamma)$ can also be introduced by a WKB method (e.g., in Ref. [39])

$$\begin{aligned} g(\gamma)&=\frac{4}{\pi\gamma}\int_0^{\tau_0}\mathrm{d}\tau\sqrt{1+\left[(s-\cosh\tau)^2-\sinh^2\tau\right]/\gamma^2}\\ &=\frac{16\sqrt{s}\sinh^2(\tau_0/2)}{\pi\gamma^2}\int_0^1\mathrm{d}u\sqrt{\frac{1-u^2}{1+\sinh^2(\tau_0/2)u^2}}. \end{aligned}$$

Obviously the result of worldline instantons technique presented here in this paper is the same as that of WKB method in Ref. [39].

It should be pointed out that the worldline instantons technique can be successfully extended to get the e^+e^- pair production rate not only in a general elliptic polarization and time alternating field [32], but also in some complex fields recently [77]. Here we just give a simple idea for the worldline instantons technique. The abundant results of e^+e^- study can be learnt more directly in the references mentioned above.

3. Pair production studied by *S*-matrix

S-matrix theory is one of the most important approaches in the perturbation framework in which the transition amplitude could be got via the initial and final states and the interaction Hamiltonian. Usually we use the Volkov states as bases to cope with the problem. As a analytical solution of quantum wave equation under a plane-wave field, the wave function of Volkov state was pioneered by Volkov [78] and further

developed by Reiss [79] and Nikishov [80]. Now it is extended to the e^+e^- study by Müller, Deneke, Hu, Keitel and Ilderton [33–37] and so on.

The solution of electrons/positrons under the external field A^μ could be well solved in terms of the known Volkov states [78,81], i.e. for electron it is $\Psi^{(e)}_{p,s} = N_p\left[1+\frac{e\not{k}\not{A}}{2(p\cdot k)}\right]u(p,s)\exp[\mathrm{i}S^{(e)}_{(p,s)}(k\cdot x)]$ and for positron it is $\Psi^{(e^+)}_{\bar{p},-\bar{s}} = N_{\bar{p}}\left[1-\frac{e\not{k}\not{A}}{2(\bar{p}\cdot k)}\right]v(\bar{p},-\bar{s})\exp[\mathrm{i}S^{(e^+)}_{(\bar{p},-\bar{s})}(k\cdot x)]$. Here $u(p,s)$ and $v(\bar{p},-\bar{s})$ are respectively the unit spinor of a free electron and a free positron, p and $\bar{p}$ the momenta, s and $\bar{s}$ the spins, and $S^{(e)}_{(p,s)}$ and $S^{(e^+)}_{(\bar{p},-\bar{s})}$ are

$$\begin{cases} S^{(e)}_{(p,s)} = -p\cdot x - \int_0^{k\cdot x}\left[\dfrac{e(p\cdot A)}{p\cdot k}-\dfrac{e^2A^2}{2(p\cdot k)}\right]\mathrm{d}\phi, \\ S^{(e^+)}_{(\bar{p},-\bar{s})} = \bar{p}\cdot x - \int_0^{k\cdot x}\left[\dfrac{e(\bar{p}\cdot A)}{\bar{p}\cdot k}+\dfrac{e^2A^2}{2(\bar{p}\cdot k)}\right]\mathrm{d}\phi. \end{cases} \tag{20}$$

We also defined the scalar four-product as $A\cdot B = A_\mu B^\mu = A_0B^0 - A_iB^i$ and $\not{A} = A_\mu\gamma^\mu$, in which γ^μ is the standard Dirac matrices. Usually the natural units, $\hbar = c = 1$, are used. Then, the amplitude for pair production process due to the collision of laser field with a high energetic gamma photon $A' = N_0\varepsilon'\exp(-\mathrm{i}k'\cdot x)$ can be calculated in the framework of first order perturbation theory as

$$\begin{aligned} S_{\mathrm{fi}} &= -\mathrm{i}e\int d^4x\ \bar{\Psi}^{(e)}_{p_\mathrm{f},s_\mathrm{f}}(x)\not{A}'(x)\Psi^{(e^+)}_{\bar{p}_i,-\bar{s}_i}(x) \\ &= -\mathrm{i}eN_{p_\mathrm{f}}N_{\bar{p}_i}N_0\int \mathrm{d}^4x\bar{u}(p_\mathrm{f},s_\mathrm{f})Mv(\bar{p}_i,-\bar{s}_i) \\ &\quad \exp\left[\mathrm{i}S^{(e^+)}(x)-\mathrm{i}S^{(e)}(x)-\mathrm{i}k'\cdot x\right], \end{aligned}$$

where M is the transition matrix elements, $S^{(e^+)}$ and $S^{(e)}$ denote $S^{(e^+)}_{(\bar{p},-\bar{s})}$ and $S^{(e)}_{(p,s)}$ respectively. In principle for given a field, we can get S_fi and then the differential cross section or/and total cross section of pair production via $\mathrm{d}\bar{\sigma}\propto\left|S_\mathrm{fi}\right|^2$.

In 2012, we have successfully made a research on e^+e^- production problem for a general elliptic polarization field by S-matrix approach [38]. We pointed out that the work is performed as a time-consuming hard task since that relatively tedious derivation of scattering amplitude and cross section was involved in the case of elliptic polarization where the scattering partial waves have many coupled terms. Fortunately, through theoretical derivation and computer calculations, we studied the case of head-on collision between a high-energy gamma photon and the laser fields, which is a typical multiphoton process of e^+e^- pair production. We first got the strict result analytically in the framework of first order perturbation theory. The obtained analytical expression can be recovered in the case of circular polarization presented in [81]. Then we got a series of numerical results for some chosen parameters thoroughly. In fact our results show that the pair creation relies strongly on the parameters of the laser fields. It is very interesting to find that the pair creation is sensitive to the elliptical polarization when the Lorentz-invariant dimensionless field strength parameter is compared to the collision energy. An important finding is that the optimal field is neither linear nor circular polarization, but is elliptical polarization in some cases.

Because too many formula appear in S-matrix theory, we have to give up a detailed description for it and suggest that the readers who are interested in S-matrix theory may refer to the articles mentioned here and references therein. The results of e^+e^- problem in elliptic polarization field can be obtained by many different research methods. For example the world-line instantons [32], S-matrix here [38], two-level transition technique [82], the following introduced DHW formalism [51,52] and so on. We point out that the results by S-matrix are coincident with those by DHW.

4. Pair production by solving QVE

Now we introduce the QVE for the study on pair production as in Refs. [24,83]. It can be derived from Dirac equation with Bogoliubov transformation. Its application conditions are limited to the case of time-dependent homogeneous electric fields [84]. In general, the source term of pair production, $s(\boldsymbol{k},t)$, obviously depends on the applied external field as well as the electron/positron kinetic property. From $\mathrm{d}f(\boldsymbol{k},t)/\mathrm{d}t = s(\boldsymbol{k},t)$, where $f(\boldsymbol{k},t)$ is the momentum distribution function of the created pairs, we get the QVE in the integro-differential equation form as

$$\frac{\mathrm{d}f(\boldsymbol{k},t)}{\mathrm{d}t} = \frac{eE(t)\varepsilon_\perp^2}{2\omega^2(\boldsymbol{k},t)}\int_{t_0}^{t}\mathrm{d}t'\frac{eE(t')[1-2f(\boldsymbol{k},t')]}{\omega^2(\boldsymbol{k},t')}\cos\left[2\int_{t'}^{t}\mathrm{d}\tau\omega(\boldsymbol{k},\tau)\right], \tag{21}$$

where the parameters are the electron/positron momentum $\boldsymbol{k} = (\boldsymbol{k}_\perp, k_\parallel(t))$, transverse energy-squared $\varepsilon_\perp^2 = m_e^2 + \boldsymbol{k}_\perp^2$, the total energy-squared $\omega^2(\boldsymbol{k},t) = \varepsilon_\perp^2 + k_\parallel(t)^2$, and the longitudinal momentum $k_\parallel(t) = k_\parallel - eA(t)$. For simplicity and also convenience of the numerical computation, it is always to transfer the original equation into the equivalent three-variable first order ordinary differential equations (ODEs) [85].

It should be emphasized that the change of QVE from the original integral-differential equation to a set of ODEs not only makes the numerical treatment simpler but also makes the involved physical quantities or/and terms clearer. Noted that the QVE reveals the Pauli exclusive principle and exhibits a typical non-Markovian character. Usually the initial conditions of ODEs can be given as zero since the field is absent at the beginning although sometimes they may have different values in terms of concrete physical problems. An important quantity is the time-dependent e^+e^- pair number density as $n(t) = 2\int\frac{\mathrm{d}^3\boldsymbol{k}}{(2\pi)^3}f(\boldsymbol{k},t)$, which is obtained by integrating the distribution function $f(\mathbf{k},t)$ in momentum or/and momenta space. It will be very useful in the following study on pair creation enhancement. Since the applied laser field becomes zero when $t\to\infty$, therefore, what we are interested in are the stationary distribution function $f = f(\boldsymbol{k}, t\to\infty)$ as well as the number density $n = n(t\to\infty)$.

4.1. Multiphoton pair production and stabilization

In our work [47], we use the electron quantities with normalized units, i.e., length $\lambda_c = \hbar/m_e c = 3.862 \times 10^{-13}$ m, momentum $m_e c = 0.511$ MeV/c, time $\tau_e = \lambda_c/c = 1.288 \times 10^{-21}$ s. In our study, some typical parameters are given, for example, the laser frequency is chosen as $\omega = 8.266 \times 10^3$ eV which corresponds to the laser wavelength $\lambda = 1.5 \times 10^{-10}$ m. The corresponding normalized laser wavelength and frequency are $\overline{\lambda} = \lambda/\lambda_c \approx 388.4$ and $\omega = 2\pi\lambda_c/\lambda \approx 0.0162$, respectively. We choose a supercycle laser pulse field as $E_1(t) = E_0 \sin(b\omega t + \varphi) e^{-(t/\tau)^{2m}}$. For simplicity, the pulse duration $\tau = 1/\omega$ is fixed with $\omega = 0.0162$ and $b \gg 1$ is an adjustable cycle parameter which meets $1/b\omega \ll \tau$ to guarantee the pulse supercycle.

In order to see the dependence of number density on the laser frequency $b\omega$, we change the cycle parameter b from 10 to 500. The results for different index m of Gaussian or super-Gaussian pulse shape are shown in Fig. 1. The created e^+e^- pairs number density is increased to some extent when m changes from 1 to 5, while the increase is not remarkable. More interesting, is that we can find clearly the multiphoton process and other rich nonlinear phenomena in pair production. On one hand, in Fig. 1 there are four pronounced jumps of the e^+e^- pair number density, denoted as I, II, III and IV, which corresponds to 1-, 2-, 3- and 4-photon process, respectively. For example, pair production can occur directly in a single photon process with a frequency $2m_e$, i.e. $b = 2/\omega = 2/0.0162 \approx 123$. The other cases with $b \approx 62$, 41 and 31 correspond to two-, three-, and four-photons processes, respectively. These multiphoton processes for pair production were also exhibited in Refs. [49,86] and our earlier work [60] in which the CQFT approach was used. On the other hand, one can see that the pair number density exhibits some small fluctuations when $b > 123$ while exhibits a monotonic decreasing when $b > 277$. The oscillation is related to the competition between two time scales, i.e., the time scale in sinusoid oscillation laser field and the time scale in Gaussian or super-Gaussian envelop field. The monotonic decreasing after a saturation is a typical nonlinear characteristic, which is very similar to the stabilization phenomenon in atomic SFI problem [87,88]. It means that the high frequency field can lead to the stabilization of the system if the laser frequency is much higher than the energy gap that makes it difficult to occur even for the single photon process. Again it should be noted that the multiphoton mechanism and phenomenon in pair production can also be obtained by the other approaches, for example, by the famous S-matrix method [38] and CQFT method [60].

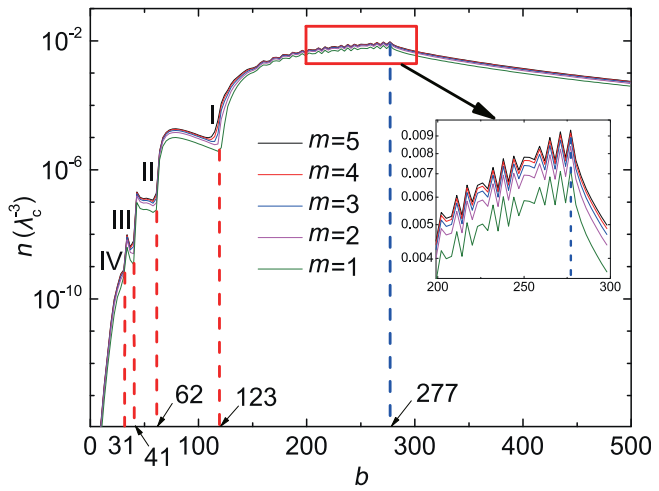

Fig. 1. The dependence of number density of created pairs with cycle parameter b in the supercycle laser electric field $E_1(t) = E_0 \sin(b\omega t + \varphi) e^{-(t/\tau)^{2m}}$ for different Gaussian or/and super-Gaussian shape with index m. The optimal pair number density locates at $b = 277$. This figure is from Ref. [47].

4.2. Multiple-slit interference effect and pair production with dynamically assisted Schwinger mechanism

In Ref. [41], authors have described a Ramsey multiple-time-slit interference effect for pairs created from the QED vacuum. They have shown that interference occurred for a sequence of alternating-sign pulses of the electric field and have proposed a qualitative description based on a study of avoided crossings in a two-level system. It is found that the central value of momentum distribution of created pairs grows like N^2 for N pulses. More about the pair production for multiple-pulse configurations can be found in Refs. [89,90]. On the other hand, it is well known that the dynamically assisted Schwinger mechanism (DASM) is very useful to improve the e^+e^- pair production rate [31], therefore, in this subsection, we will show our work recently [48] on the e^+e^- pair production study by solving QVE through combining the multiple-slit interference effect with the DASM scheme.

The problem is considered in the presence of the electric field

$$\begin{aligned} E(t) &= E_1(t) + E_2(t) \\ &= \sum_{i=0}^{N-1} (-1)^i E_1 \mathrm{sech}^2[\omega_1(t - i\cdot\tau_1)] \\ &\quad + \sum_{i=0}^{N-1} (-1)^i E_2 \mathrm{sech}^2[\omega_2(t - i\cdot\tau_2 + T)], \end{aligned} \tag{22}$$

where N is the electric field pulse number, $E_{1,2}(t)$ denotes a strong/weak and slowly/rapidly varying alternating-sign electric field pulse train, $E_{1,2}$ is the electric field strength, $\omega_{1,2}$ represents the inverse-time width scale, $\tau_1 = \tau_2 \equiv \tau$ is the time delay between the electric field pulses, and T is the time interval between the electric fields $E_1(t)$ and $E_2(t)$. For convenience, we choose $E_1 = 0.1$, $\omega_1 = 0.02$, $E_2 = 0.01$, and $\omega_2 = 0.22$. A typical combined field $E(t)$ is plotted in Fig. 2.

What we are interested in is the dependence of the number density of created particles $n[\boldsymbol{k}_\perp = 0]$ on the electric field pulse number N. The result is shown in Fig. 3 for the electric fields of $E_1(t)$ (blue triangles), $E_2(t)$ (red circles), and the combined $E(t)$ (black squares), respectively. The dotted blue, dashed red and

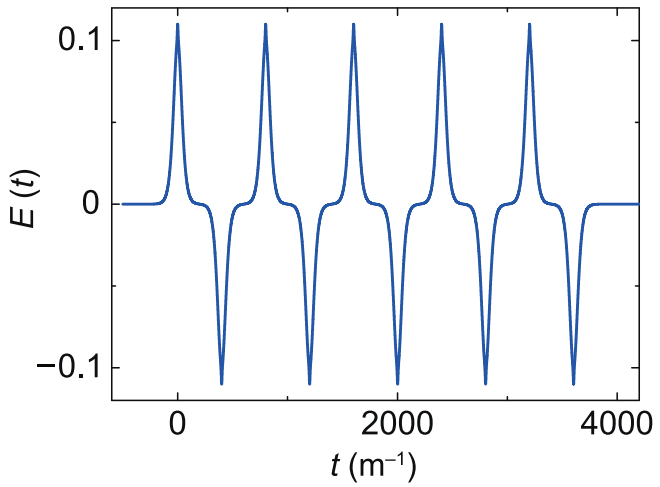

Fig. 2. A typical combined electric field $E(t)$ with $N = 10$. The electric field parameters are chosen as $E_1 = 0.1$, $\omega_1 = 0.02$, $E_2 = 0.01$, $\omega_2 = 0.22$, $\tau = 400.3$, and $T = 0$. This figure is from Ref. [48].

solid black lines are the fitted ones for $E_1(t)$, $E_2(t)$ and $E(t)$ with the slopes ~0.758, 0.775 and 1.609, respectively. A reference solid green line $n[\boldsymbol{k}_\perp = 0] \propto N^2$ is also shown. One can see that the number density of created particles increases by a power law with N varying from 1 to 10 in the three cases of $E_1(t)$, $E_2(t)$ and $E(t)$. Obviously this law is complex and different from that between the central momentum distribution function and the pulse number. Moreover, we can also see that the number of created particles can be greatly enhanced by combining the multiple-slit interference effect with the DASM. This result concludes that in order to get a large particle number density, it is better to combine the interference effect with the DASM than just increasing the pulse number N [48].

We also researched the number density of created particles $n(+\infty)$ depending on the pulse number N in the full momentum space, which are shown in Fig. 4 for the electric fields of $E_1(t)$ (dotted blue line), $E_2(t)$ (dashed red line), and the combined $E(t)$ (solid black line), respectively. It is found that the e^+e^- number density $n(+\infty)$ grows with N, and the e^+e^- pair production is highly enhanced by combining the multiple-slit interference effect with the DASM. Moreover, it is also found that there is still power law of the number density $n(+\infty)$ depending on the pulse number N by including the transverse momentum $\boldsymbol{k}_\perp$. However, the index 1 of power law, which is different from that shown in Fig. 3, means that the number density $n(+\infty)$ depends linearly on the pulse number N in the case of full momenta consideration. It is noted that, although the momentum region of pair production shrinks with N, the contribution of transverse momentum is obvious because it affects the total number of created particles a lot.

The enhancement of pair creation shown in Figs. 3 and 4 can be understood physically from two aspects. On one hand, the rapidly varying electric field can generate many transient states between positive and negative states in Dirac vacuum, which will increase additional seeds for the Schwinger mechanism [31]. On the other hand, in the scattering picture, the alternating-sign field pulse train can cause the resonant tunneling [45]. This will open more channels for creating e^+e^- pairs, i.e., will enhance Schwinger pair production.

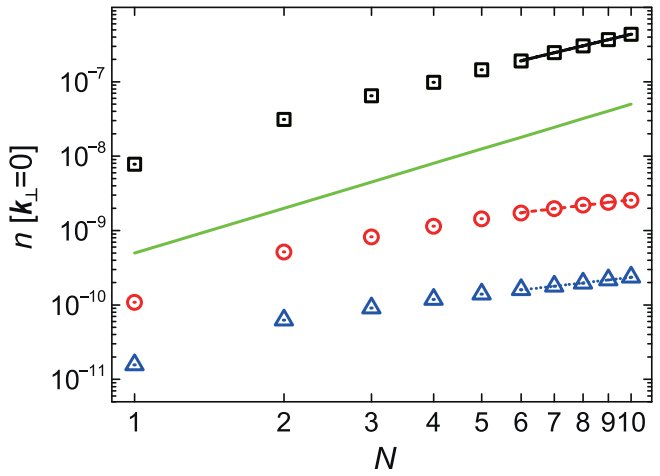

Fig. 3. The number density of created pairs $n[\boldsymbol{k}_\perp = 0]$ *vs* pulse number N, for the electric fields of $E_1(t)$ (blue triangles), $E_2(t)$ (red circles), and the combined $E(t)$ (black squares), respectively. The dotted blue, dashed red and solid black lines are the fitted ones for $E_1(t)$, $E_2(t)$ and $E(t)$ with the slopes ~0.758, 0.775 and 1.609, respectively. The solid green line is a reference one as $n[\boldsymbol{k}_\perp = 0] \propto N^2$. The other field parameters can be found in the text. This figure is from Ref. [48].

5. Pair production in the DHW formalism

Let us turn to the study on the pair production in more complex and realistic fields by using a stronger theoretical tool, i.e., DHW formalism. The DHW formalism has been used to study vacuum pair production in Refs. [91–93] for different electric fields. The advantages by DHW are that it can not only reveal many novel signatures for understanding the complicated physics in pair production but also help to guide the possible future experimental realization.

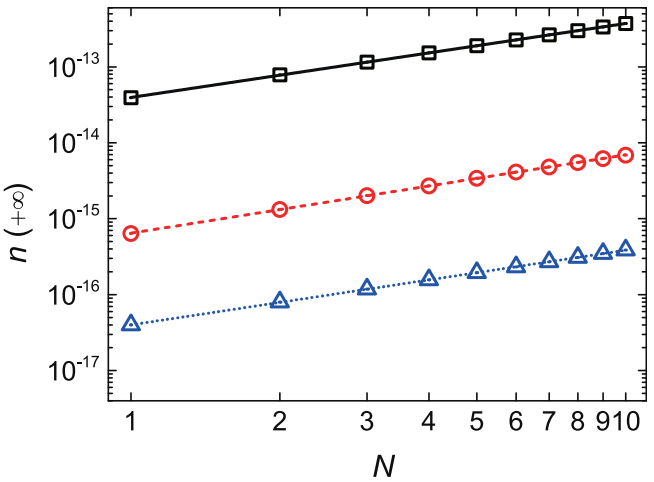

Fig. 4. The number density of created pairs $n(+\infty)$ *vs* pulse number N, for the electric fields of $E_1(t)$ (dotted blue line), $E_2(t)$ (dashed red line), and the combined $E(t)$ (black solid line), respectively. The electric field parameters are the same as in Fig. 2. This figure is from Ref. [48].

Among existed studies, the polarization of fields is concerned. For example, for a linearly polarized electric field, the momentum spectrum of created e^+e^- pairs in laser pulses with subcycle structures are investigated in Ref. [45]. It is found that the longitudinal momentum spectrum is extremely sensitive to the laser field parameters and its oscillations can be used as a probe of subcycle structures in ultrashort laser pulses. For a circularly polarized electric field that only changes with time, Schwinger pair production is explored numerically with the real-time DHW formalism in Ref. [50]. It is found that the characteristic momentum distribution in this field might be used to distinguish a QED cascade seeded by pair production from that seeded by isotropic vacuum impurity. In Ref. [49], e^+e^- pair production in nonperturbative multiphoton regime is studied and the effective mass signatures are identified. Furthermore, the pair creation rate for rotating electric fields is also investigated semiclassically with the WKB approximation in Ref. [43]. It is found that for a certain range of electric field parameters, the pair production rate is dominated by one spin of created pairs. More recently, the pair production in simple electric and magnetic fields is studied with DHW formalism in Ref. [94]. It is found that the magnetic field will suppress the pair creation process.

We have performed some primary studies about the e^+e^- pair production for a general elliptic polarization field, for example, we studied analytically the leading term of pair production by using the worldline instanton method [32], the *S*-matrix method [38] and also a two-level transition technique [82], respectively. However the study by DHW can still give more highlights on this problem as seen below.

First we give a brief description for DHW formalism. Although DHW can cope with variable spatial- and temporal-field simultaneously, as in QVE, we just consider the spatially homogeneous and time-dependent fields and focus on the e^+e^- pair production in a uniform and time-varying electric field of arbitrary polarization as

$$\boldsymbol{E}(t)=\frac{E_0}{\sqrt{1+\delta^2}}\exp\left(-\frac{t^2}{2\tau^2}\right)\begin{bmatrix}\cos(\omega t+\phi)\\ \delta\sin(\omega t+\phi)\\ 0\end{bmatrix}, \tag{23}$$

where E_0 is the field amplitude, τ defines the pulse duration, ω is the laser frequency, ϕ is the carrier-envelope phase, and $|\delta|\le 1$ represents the polarization (or the ellipticity). For convenience, we set $\phi=0$ and $\delta>0$ unless otherwise specified. A similar electric field with the polarization up to ± 0.93 has been actually achieved experimentally [98] while the intensity is low.

For simplicity, we start with the equal-time density operator of two Dirac field operators in the Heisenberg picture,

$$\widehat{\mathcal{C}}_{\alpha\beta}(\boldsymbol{x},\boldsymbol{y},t)=\mathrm{e}^{-\mathrm{i}e\int_{-1/2}^{1/2}\boldsymbol{A}(\boldsymbol{x}+\lambda\boldsymbol{y},t)\cdot\boldsymbol{y}\mathrm{d}\lambda}\times\left[\widehat{\Psi}_\alpha\left(\boldsymbol{x}+\frac{\boldsymbol{y}}{2},t\right),\ \widehat{\overline{\Psi}}_\beta\left(\boldsymbol{x}-\frac{\boldsymbol{y}}{2},t\right)\right], \tag{24}$$

with the center-of-mass coordinate $\boldsymbol{x}=(\mathbf{x}_1+\boldsymbol{x}_2)/2$ and the relative coordinate $\boldsymbol{y}=\boldsymbol{x}_1-\boldsymbol{x}_2$. Note that the factor before the commutator is a Wilson-line factor used to keep gauge invariance, and the integration path of the vector potential $\boldsymbol{A}$ is a straight line chosen to introduce a clearly defined kinetic momentum $\boldsymbol{p}$. Moreover, we have employed a Hartree approximation for the electromagnetic field and chosen the temporal gauge $A_0=0$. The Wigner operator is defined as the Fourier transformation of Eq. (24) with respect to the relative coordinate $\boldsymbol{y}$, and its vacuum expectation value gives the Wigner function

$$\mathcal{W}(\boldsymbol{x},\boldsymbol{p},t)=-\frac{1}{2}\int \mathrm{d}^3y\mathrm{e}^{-\mathrm{i}\boldsymbol{p}\cdot\boldsymbol{y}}\langle 0|\widehat{\mathcal{C}}(\boldsymbol{x},\boldsymbol{y},t)|0\rangle. \tag{25}$$

Decomposing the Wigner function in terms of a complete basis set $\left\{1,\gamma_5,\gamma^\mu,\gamma^\mu\gamma_5,\sigma^{\mu\nu}:=\frac{\mathrm{i}}{2}[\gamma^\mu,\gamma^\nu]\right\}$, we have

$$\mathcal{W}(\boldsymbol{x},\boldsymbol{p},t)=\frac{1}{4}(\mathbb{1}\mathbb{s}+\mathrm{i}\gamma_5\mathbb{p}+\gamma^\mu\mathbb{v}_\mu+\gamma^\mu\gamma_5\mathbb{a}_\mu+\sigma^{\mu\nu}\mathbb{t}_{\mu\nu}), \tag{26}$$

with sixteen real Wigner components, i.e., scalar $\mathbb{s}(\boldsymbol{x},\boldsymbol{p},t)$, pseudoscalar $\mathbb{p}(\boldsymbol{x},\boldsymbol{p},t)$, vector $\mathbb{v}(\boldsymbol{x},\boldsymbol{p},t)$, axial vector $\mathbb{a}(\boldsymbol{x},\boldsymbol{p},t)$, and tensor $\mathbb{t}(\boldsymbol{x},\boldsymbol{p},t)$. Inserting the decomposition into the equation of motion for the Wigner function, one can obtain a partial differential equation (PDE) system for the sixteen Wigner components [91]. Furthermore, for the spatially homogeneous and time-dependent electric fields mentioned above, by using the method of characteristics, or simply, replacing the kinetic momentum $\boldsymbol{p}$ by $\boldsymbol{q}-e\boldsymbol{A}(t)$ with the well-defined canonical momentum $\boldsymbol{q}$, the PDE system for the sixteen Wigner components can be reduced to an ODE system for the ten nontrivial Wigner components $\mathbb{w}(\boldsymbol{q},t)=(\mathbb{s},\mathbb{v},\mathbb{a},\mathbb{t}_1:=2\mathbb{t}^{i0}\boldsymbol{e}_i)^{\mathrm{T}}(\boldsymbol{q},t)$,

$$\dot{\mathbb{w}}(\boldsymbol{q},t)=\mathcal{H}(\boldsymbol{q},t)\mathbb{w}(\boldsymbol{q},t), \tag{27}$$

where the dot denotes a total time derivative, and $\mathcal{H}(\boldsymbol{q},t)$ is a 10×10 matrix.

The one particle distribution function is defined as

$$f(\boldsymbol{q},t)=\frac{1}{2}\mathbb{e}_1^{\mathrm{T}}\cdot[\mathbb{w}(\boldsymbol{q},t)-\mathbb{w}_{\mathrm{vac}}(\boldsymbol{q},t)], \tag{28}$$

where $\mathbb{w}_{\mathrm{vac}}(\boldsymbol{q},t)=(\,\mathbb{s}_{\mathrm{vac}}\quad\mathbb{v}_{\mathrm{vac}}\quad 0\quad 0\,)^{\mathrm{T}}$, $\mathbb{s}_{\mathrm{vac}}=-2m/\Omega(\boldsymbol{p})\big|_{\boldsymbol{p}\to\boldsymbol{q}-e\boldsymbol{A}(t)}$, $\mathbb{v}_{\mathrm{vac}}=-2\boldsymbol{p}/\Omega(\boldsymbol{p})\big|_{\boldsymbol{p}\to\boldsymbol{q}-e\boldsymbol{A}(t)}$, $\Omega(\boldsymbol{p})\big|_{\boldsymbol{p}\to\boldsymbol{q}-e\boldsymbol{A}(t)}=\{m^2+[\boldsymbol{q}-e\boldsymbol{A}(t)]^2\}^{1/2}$ is the total energy of electrons, and $\mathbb{e}_1=-1/2\,\mathbb{w}_{\mathrm{vac}}$ is one of the basis of the ten-component vector $\mathbb{w}$. Notice that the vacuum solution is $\mathbb{w}_{\mathrm{vac}}(\boldsymbol{q},t_{\mathrm{vac}})$.

In order to precisely obtain the distribution function f, we employ the method used in Ref. [50]. Decomposing the Wigner components as $\mathbb{w}=2(f-1)\mathbb{e}_1+\mathcal{F}\mathbb{w}_9$ with an auxiliary nine-component vector $\mathbb{w}_9$ and a 10×9 matrix $\mathcal{F}=\begin{pmatrix}-\boldsymbol{p}^{\mathrm{T}}/m & 0\\ \mathbb{1}_9\end{pmatrix}\Big|_{\boldsymbol{p}\to\boldsymbol{q}-e\boldsymbol{A}(t)}$, and applying Eq. (27), we have

$$\begin{aligned} \dot{f} &= 1/2\ \dot{e}_1^T \mathcal{F} \mathbb{w}_9, \\ \dot{\mathbb{w}}_9 &= \mathcal{H}_9 \mathbb{w}_9 + 2(1-f)\mathcal{G}\dot{e}_1, \end{aligned} \tag{29}$$

where $\mathcal{G} = (0 \quad \mathbb{1}_9)$ is a 9×10 matrix, and

$$\mathcal{H}_9 = \begin{pmatrix} -e\boldsymbol{p}\cdot\boldsymbol{E}^{\mathrm{T}}/\omega^2(\boldsymbol{p}) & -2\boldsymbol{p}\times & -2m \\ -2\boldsymbol{p}\times & 0 & 0 \\ 2(m^2+\boldsymbol{p}\cdot\boldsymbol{p}^{\mathrm{T}})/m & 0 & 0 \end{pmatrix}\Big|_{\boldsymbol{p}\to\boldsymbol{q}-e\boldsymbol{A}(t)}.$$

Thus, we can get the one particle momentum distribution function $f(\boldsymbol{q},t)$ by solving Eq. (29) with the initial conditions $f(\boldsymbol{q},-\infty) = \mathbb{w}_9(\boldsymbol{q},-\infty) = 0$. Integrating the distribution function over full momenta at $t \to +\infty$, we have the number density of created pairs

$$n(+\infty) = \int \frac{\mathrm{d}^3 q}{(2\pi)^3} f(\boldsymbol{q},+\infty). \tag{30}$$

As mentioned earlier in this paper, when $\gamma \ll 1$ the tunneling process, i.e. nonperturbative Schwinger pair production, dominates pair production, and when $\gamma \gg 1$ the main contribution to pair creation comes from multiphoton mechanism that results in the perturbative multiphoton pair creation. However, when $\gamma \sim \mathcal{O}(1)$, i.e. nonperturbative multiphoton regime [95], multiphoton pair production will have a nonperturbative signature in which many interesting features will take place [49,95,96], also seen in our study below.

5.1. Polarization effect

By solving Eq. (37) numerically, the momentum spectra of created particles in the polarization plane (q_x,q_y) can be obtained for different polarizations with $\gamma = 0.35\sqrt{1+\delta^2}$ (Fig. 5). From Fig. 5(a), one can see clearly the oscillatory structures of momentum spectrum. This result is similar to the one in Ref. [45], because for $\delta = 0$ our electric field Eq. (31) will become the linearly polarized field as in Ref. [45]. When $\delta \neq 0$, however, the oscillations vanish and the peak position of momentum distribution shifts along the direction of q_y (see Fig. 1(b)). When δ increases, the momentum distribution of created e^+e^- pairs would distorted gradually until it forms a ring-like structure when $\delta \sim 1$. Another interesting phenomenon is that the interference effects in momentum distribution disappears in this few-cycle field ($\sigma = \omega\tau = 5$). We think the reason is that the polarization changes the distribution of turning points which results in only one pair of turning points dominating the pair creation. It should also be noted that the odd electric field component $E_y(t)$ causes the momentum distribution asymmetric as $q_y = 0$ [97], which is similar to Fig. 4 of Ref. [45].

Now let us study and discuss the relation between the structure of the momentum distribution and field parameters. Based on the analysis in Ref. [50], it is known that for a circularly polarized field, the circular distortion of momentum

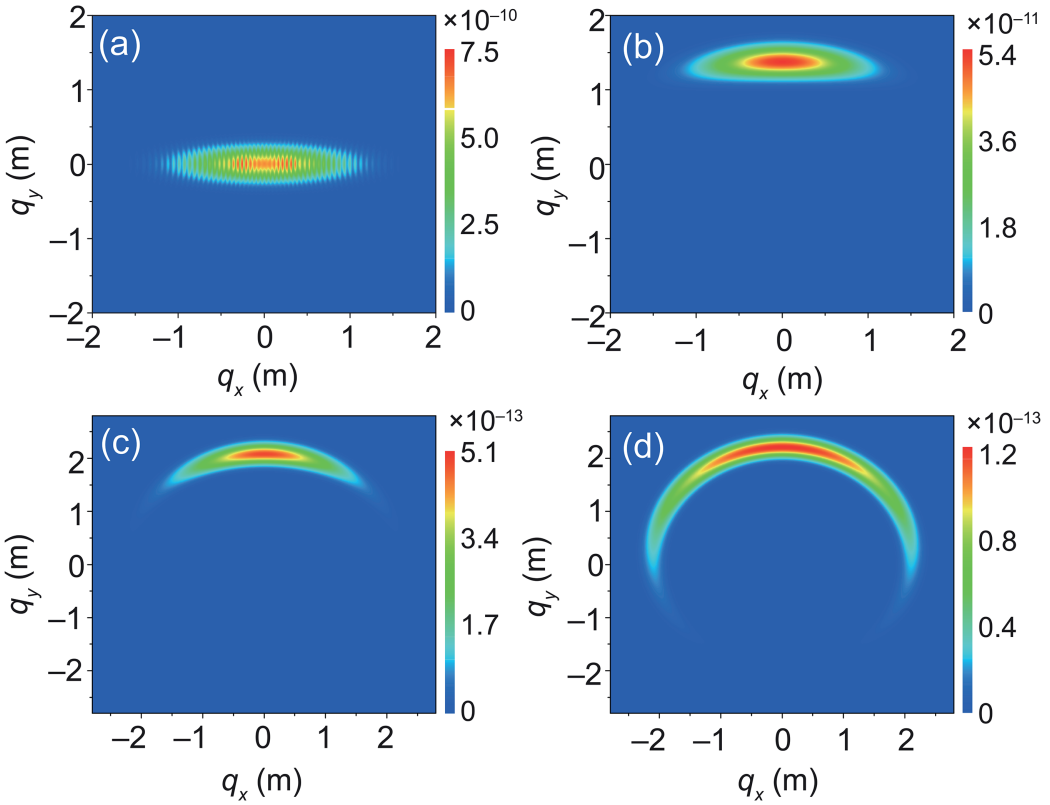

Fig. 5. Momentum spectra of created e^+e^- pairs in the (q_x, q_y) plane for different polarizations of (a) $\delta = 0$, (b) $\delta = 0.5$, (c) $\delta = 0.9$, and (d) $\delta = 1.0$. Other electric field parameters are chosen as $E_0 = 0.1\sqrt{2}E_{\mathrm{cr}}$, $\omega = 0.05\ m$ and $\tau = 100/m$. This figure is from Ref. [51].

distribution can be enhanced by increasing the pulse duration, because the produced particles have enough time to follow the rotation of this field. When the circularly distorted momentum distribution closes into a ring, interference effects will occur. An intuitively plausible understanding about this is that the quantum wave functions of left-moving and right-moving particles carrying different phases will superpose each other and induce quantum interference. In fact, in terms of our study, this effect can not be fully understood just by using circularly polarized fields and the explanation of superposition of quantum wave functions of left-moving and right-moving particles is not adequate.

In order to answer this problem, we increase the cycle number of electric field ($\sigma = 15$) by increasing the pulse duration and plot the momentum spectra of created pairs for different polarizations in Fig. 6. Indeed, as discussed above, we can see a ring-like structure and the interference effect in the momentum spectrum for $\delta = 1$ (see Fig. 6(c)). However, surprisingly we also find that for a small value of δ, the particle distribution in momentum space splits into two segments in the q_y direction and interference effects still exist in each segment. This result indicates clearly that the interference effect is related to the cycle number of electric field. Actually, it is caused by the interference among different pair-creation amplitudes corresponding to different turning points in the complex t plane [43]. Thus, for a many-cycle field, there will be many pairs of turning points having nearly the same distance to the real t axis and this can induce evident interference effect [97]. Consequently, the interference effect in momentum spectrum will become more and more remarkable with the cycle number increasing.

Since the maximum value of the momentum distribution function $f(+\infty)$ decreases with polarization, one expects to conclude that the number density of created e^+e^- pairs may have the same dependence relation. However, things are more complicated than the expectation.

To clarify the number density *vs* the field polarization, the number density scanning over the field frequency, for different polarizations is shown in Fig. 7. It is found that there are many obvious oscillations on the curves and these oscillations in the small frequency region vanish gradually as the polarization increases. In fact these oscillations caused by multiphoton pair production have been studied for a linearly polarized field in Refs. [47,49]. Additionally, we also find that for a small field

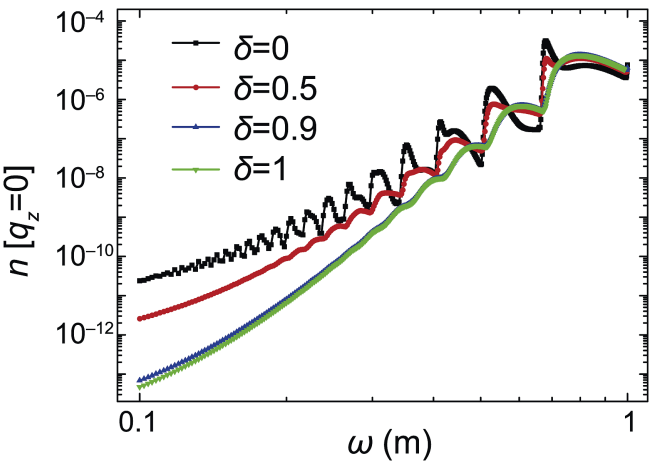

Fig. 7. The number density of created particles $n[q_z=0]$ *vs* frequency ω for different polarizations of $\delta = 0$, 0.5, 0.9, and 1, respectively. Other electric field parameters are the same as in Fig. 5. This figure is from Ref. [51].

frequency the number density of created particles decreases greatly with the polarization. This is attributed to that, for small laser frequencies, nonperturbative Schwinger pair production is more significant. As pair creation is suppressed exponentially for weak fields, the number density is dominated by the electric field component with a large amplitude. Therefore, the polarized field of small δ has a larger amplitude of field component than that of large δ, which results in a high number density.

On the other hand, for large field frequencies, it is found that the relation between the number density and the polarization of electric field becomes more complicated, because the perturbative multiphoton process becomes more important. To see this point clearly, we also plot the number density as a function of polarization for different laser frequencies in Fig. 8. It can be seen clearly that the number density of created pairs can reach its maximum at $\delta = 0$, $\delta = \pm 1$, or even $0 < |\delta| < 1$ for different field frequencies. Thus, for a large laser frequency the relation between the particle number density and the polarization of electric field is sensitive to the field frequency.

In a word, we calculate the momentum spectrum and the number density of created particles in different polarized electric fields with the same laser intensity and consider the effects of field polarizations on them. We find that, as

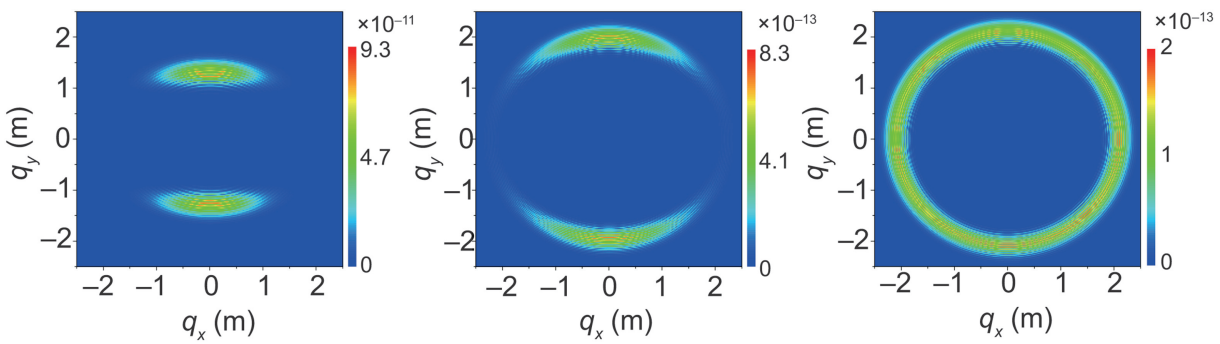

Fig. 6. Momentum spectra of created e^+e^- pairs in the (q_x, q_y) plane for different polarizations of $\delta = 0.5$, 0.9, and 1, respectively (from left to right). Other electric field parameters are chosen as $E_0 = 0.1\sqrt{2}E_{cr}$, $\omega = 0.05\ m$ and $\tau = 300/m$. This figure is from Ref. [51].

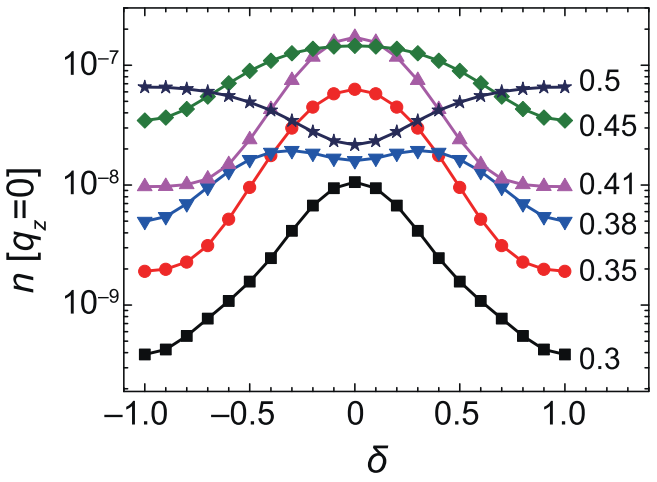

Fig. 8. The number density of created particles $n[q_z=0]$ *vs* polarization δ for different field frequencies. Other electric field parameters are the same as in Fig. 5. This figure is from Ref. [51].

polarization increases, the circular distortion of momentum distribution becomes more obvious for few-cycle fields, while the momentum spectra split for many-cycle fields. It is also found that the particle number density deceases with polarization for a small laser frequency while the relation between them is more complicated for a large laser frequency. These results are expected to be helpful for the understanding of e^+e^- pair creation in complex fields. The results presented here may also be used to build an intimate bridge between vacuum e^+e^- pair creation and SFI study.

5.2. Nonperturbative multiphoton signatures in pair production

By observing the detailed node structures of momentum spectra, it is found that the even-number photon pair production is absent in a certain of parameters. We think it is a typical one of nonperturbative multiphoton signatures in e^+e^- pair production. Now a typical result about the dependence of distribution function $f(+\infty)$ on the laser frequency is shown in Fig. 9 for a general elliptic polarization field.

From Fig. 9(a), a case of linearly polarized field $\delta = 0$, it is found that when $q_x = 0$ (x denotes the direction of external field), there is no even-number photon pair creation, see the black solid-line. This result can be explained quantitatively that when $q_x = 0$, one has an expression $f \propto [1+(-1)^{n+1}]$ for e^+e^- pair production, see Eq. (3) of Ref. [52] in detail. Obviously, when n is even number, f vanishes, which shows that the momentum distribution function becomes zero for even-number photon pair creation. Our new findings are that the similar vanishing of even-number photon pair creation occur also for $\delta \neq 0$, see Fig. 9(b) and (c), but the conditions are limited to the cases of $q_x = q_y = 0$. In our study, we successfully explained this nontrivial results by applying Eq. (3) of Ref. [52], but the momentum q_x is reasonably replaced with $(q_x^2 + q_y^2)^{1/2}$.

Another understanding of the vanishing of even-number photon pair creation is seen from the C-parity selection rule [95]. It seems to be a more physical interpretation assumed that the orbital angular momentum (OAM) of created pairs l is associated with q_x. The odd or even l lead to the even or odd C-parity and the selection rule determines whether the even-number photon pair creation occurs. If this assumption holds, it would be a useful technique to detect the OAM information by analyzing the momentum spectra of the created particles for the first time. Certainly it is a theoretical conclusion and its validation needs experimental verification in the future.

Moreover, from Fig. 9, one can see some oscillations on the left side of n-photon peaks. This is caused by the combined effect between Schwinger mechanism and multiphoton pair production. It is known that a field frequency which is less than the resonant frequency is unable to overcome the threshold of pair creation $2m_*$. However, for some frequencies, a negative-energy electron in the Dirac sea can be stimulated to an intermediate state and become a positive-energy electron by the tunneling process. Therefore, there will present some peaks of the distribution function for these frequencies. Noted that the resonance phenomena on pair production are reduced gradually and even disappears with δ. In particular there remains only one photon pair creation when $\delta = 1$.

Through the careful study we find that there exists abundant signatures of created particles in momentum spectrum. Not only possibly the OAM information of created particles can be detected by them but also some signatures of ultrashort laser pulses can be extracted, for example, the frequency information. In fact, many works about the momentum structure depending on the field parameter have been found in atomic ionization study (see Refs. [98–100]). So we believe that the phenomena presented in e^+e^- pair production here are expected to be observed more easily in atom ionization for general elliptical polarized laser pulses. It bridges a same physical mechanism behind the similar phenomena between e^+e^- pair production in an ultrastrong laser field and atomic ionization in an intense laser field.

6. Pair production in terms of CQFT

Finally, we introduce another important approach named CQFT which is mainly developed by Su and Grobe et al. [53–58] and then widely explored by many others [59,60].

The idea of CQFT is that the Dirac equation [101,102] governs an evolution of the field $\widehat{\psi}(z,t)$ as

$$\mathrm{i}\partial\widehat{\psi}(z,t)/\partial t = \left[c\alpha_z\widehat{P} + \beta c^2 + V(z,t)\right]\widehat{\psi}(z,t), \tag{31}$$

where α_z and β are the z component and diagonal parts of the spin Dirac matrix, respectively, c is the light speed of vacuum and $V(z,t)$ is the scalar potential of applied field. The atomic units $\hbar = e = m_e = 1$ are used usually in CQFT. In terms of the creation and annihilation operators, one can express $\widehat{\psi}(z,t)$ as follows

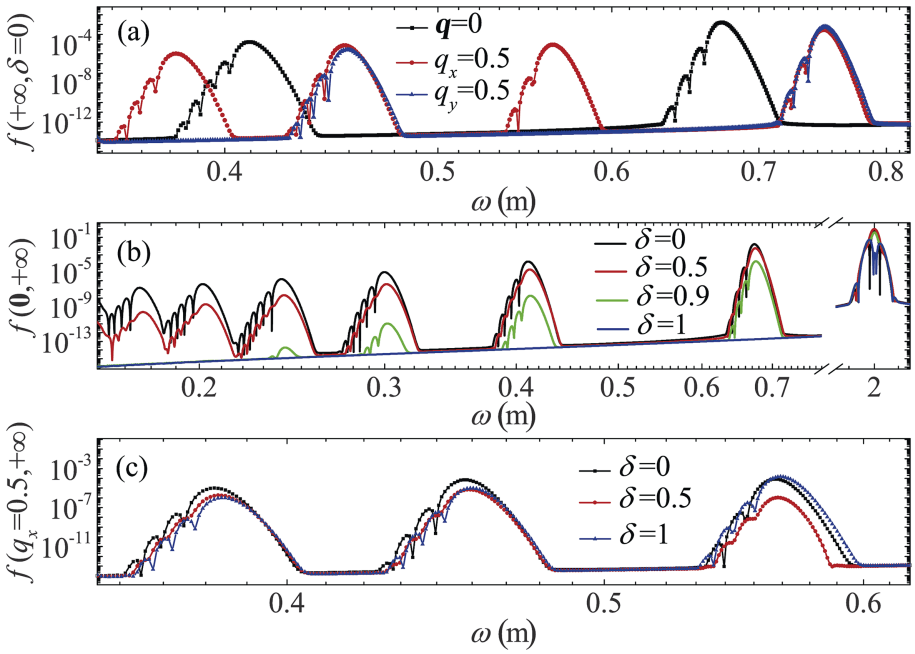

Fig. 9. A function of $f(+\infty)$ with ω when $E_0 = 0.1\sqrt{2}E_{cr}$. (a) is the case of linearly polarized electric field, i.e. $\delta = 0$, for different momenta $\boldsymbol{q}$. (b) is the case of zero momentum, i.e. $\boldsymbol{q} = 0$ for different polarizations δ, which are 0, 0.5, 0.9, and 1 from top to bottom. (c) is the case of nonzero momentum, $q_x = 0.5$ but $q_y = q_z = 0$, for different polarizations δ, which are 0, 0.5, and 1 from top to bottom. This figure is from Ref. [52].

$$\widehat{\psi}(z,t) = \sum_p \widehat{b}_p(t)W_p(z) + \sum_n \widehat{d}_n^{\dagger}(t)W_n(z) = \sum_p \widehat{b}_p W_p(z,t) + \sum_n \widehat{d}_n^{\dagger} W_n(z,t), \tag{32}$$

where $\sum_p$ and $\sum_n$ denote summation or/and integration over all positive and negative states, respectively. Meanwhile $W_p(z,t) = \langle z|p(t)\rangle$ and $W_n(z,t) = \langle z|n(t)\rangle$ are the solutions of the Dirac equation for the initial conditions of $W_p(z,t{=}0) = W_p(z)$ and $W_n(z,t{=}0) = W_n(z)$, respectively, where these initial states are the corresponding positive and negative energy eigenfunctions of the field-free Dirac equation.

With the help of Eq. (32), one can express the fermion operators as

$$\widehat{b}_p(t) = \sum_{p\prime} \widehat{b}_{p\prime} U_{pp\prime}(z,t) + \sum_{n\prime} \widehat{d}_{n\prime}^{\dagger} U_{pn\prime}(z,t), \tag{33}$$

$$\widehat{d}_n^{\dagger}(t) = \sum_{p\prime} \widehat{b}_{p\prime} U_{np\prime}(z,t) + \sum_{n'} \widehat{d}_{n\prime}^{\dagger} U_{nn\prime}(z,t), \tag{34}$$

$$\widehat{b}_p^{+}(t) = \sum_{p'} \widehat{b}_{p'}^{\dagger} U_{pp'}^{*}(z,t) + \sum_{n'} \widehat{d}_{n\prime} U_{pn\prime}^{*}(z,t), \tag{35}$$

$$\widehat{d}_n(t) = \sum_{p'} \widehat{b}_{p'}^{\dagger} U_{np'}^{*}(z,t) + \sum_{n'} \widehat{d}_{n\prime} U_{nn\prime}^{*}(z,t), \tag{36}$$

where $U_{p(n)p'(n')} = \langle p(n)|p'(n')(t)\rangle$. Their meanings can be seen firstly by solving the force-free Dirac wave equation as one can get the eigenstates $|p'(n')\rangle$, and then by projecting them to all states $|p(n)\rangle$. A useful quantity is the density of the created electrons $\rho_e = \langle \mathrm{vac}|\widehat{\psi}^{(+)\dagger}(r,t)\widehat{\psi}^{(+)}(r,t)|\mathrm{vac}\rangle$, where $\widehat{\psi}^{(+)}$ is the positive frequency part of the field operator. In one dimensional case, the number $N(t) = \int \mathrm{d}z\rho_e$ of the created pairs can be got. In fact, from the analysis mentioned above we have

$$\rho_e = \sum_n \Big|\sum_p U_{pn}(t)W_p(z)\Big|^2, \tag{37}$$

and

$$N(t) = \sum_p \langle \mathrm{vac}|b_p^{\dagger}(t)b_p(t)|\mathrm{vac}\rangle = \sum_p \sum_n |U_{pn}(t)|^2. \tag{38}$$

Then the momentum spectrum of the created pairs is also conveniently got as

$$\rho_p = \sum_n |U_{pn}(t)|^2. \tag{39}$$

Now let us turn to the evolution of the states. Usually it is realized numerically by using a well known split-operator technique [53]. The whole evolution time is assumed to be T with N_t time steps. The whole calculated spatial scale is the length of L with N_z grid points. Thus the evolution operator in each time step can be written as

$$\begin{aligned} U(t+\Delta t,t) &= \widehat{T}\exp\left\{-\mathrm{i}\int_t^{t+\Delta t}[h_0 + V(z,t)]\mathrm{d}t\right\} \\ &= \exp\{-\mathrm{i}[h_0 + V(z,t+\Delta t/2)]\Delta t\} + O(\Delta t^3) \\ &= \exp(-\mathrm{i}V\Delta t/2)\exp(-\mathrm{i}h_0\Delta t)\exp(-\mathrm{i}V\Delta t/2) \\ &\quad + O(\Delta t^3), \end{aligned} \tag{40}$$

where h_0 is the Hamiltonian with no field. The matrix elements $U_{pn}(t)$ can be got through adopting the fast Fourier transformation technique to Eq. (40).

As an illustration of CQFT, we just give a partial presentation of results in our work [60], where we have investigated the momentum spectrum of the created pairs. A simple scaling law for the multiphoton process is found.

The total field is constituted by a symmetric potential well and an alternating field as $V(z, t) = V_1S(z)f(t) + V_2\sin(\omega t)S(z)\theta(t; t_0, t_0 + t_1)$, where $S(z) = \{\tanh[(z-D/2)/W]-\tanh[(z+D/2)/W]\}/2$ with the potential-well field width D and extension W at each edge. The function $f(t) = \sin(\pi t/2t_0)\theta(t; 0, t_0) + \theta(t; t_0, t_0+t_1) + \cos[\pi(t - t_0 - t_1)/2t_0]\theta(t, t_0 + t_1, 2t_0 + t_1)$ works in the turn-on and -off processes of the potential-well with the unit-step-function $\theta(t; t_1, t_2)$ when time is between t_1 and t_2. Noted that during $0 < t < t_0$ the potential well exists but it is turned off at $t = t_0 + t_1$. Since the turning on and off has a strong effect on pair creation [58], a long duration $t_0 = 5/c^2$ has to be used for reducing the possible temporal influence. In our study, we chose the duration of the oscillating field as $(t_0, t_0 + t_1)$ with $t_1 = 20\pi/c^2$ as a few times of laser period. The behavior of potential $V(z, t)$ can be seen in Fig. 10.

As an example, a typical momentum density distribution of the created electrons is shown in Fig. 11. The parameters are chosen as follows: potential well depth $V_1 = 2c^2-10{,}000$ with width $D = 10\lambda_e$ which is 10 times of the Compton wavelength λ_e, oscillating potential amplitude $V_2 = 2c^2-10{,}000$ with frequency $\omega = 2.1c^2$. An obvious phenomenon is the momentum distribution symmetry in this figure.

As shown in Fig. 11(a), one can see that the produced electrons are grouped when they are created and can absorb different numbers of photons in the potential well. Corresponding to the multiphoton processes involving different numbers of photons in Fig. 11(b)–(d), we marked clearly the concrete value of the momentum for each peak, which would be very helpful to get the law of multiphoton absorption in the following.

The simplest one photon process is shown in Fig. 11(b), where the presented results can lead a simple relation $E_{pi} = E_i + \omega$ between the energy of the created electrons momentum-peak E_{pi} and the energy levels of electrons in potential well E_i. These two energies can be determined by the formula of $E^2 = p^2 + c^4$ with $p = 2\pi N_p/L$ and $cp_2\cot(p_2D) = EV_1/cp_1-cp_1$ [102], respectively, where N_p is the peak number and $L = 2.0$ is the length of the numerical grid, and $p_2 = \sqrt{(E + V_1)^2/c^2 - c^2}$ and $p_1 = \sqrt{c^2 - E^2/c^2}$. The values of E_{pi} and E_i for the 8 peaks of $N_p = 58$, 65, 71, 83, 95, 107, 118, 127 are shown in Table 1. By analyzing them, one can easily get the law of $E_{pi} = E_i + \omega$ which embodies the one-photon pair creation process.

On the other hand, for those peaks of $N_p = 9$, 33, 39, 47, the corresponding energies are $E_{N_p=9} = 1.25c^2$, $E_{N_p=33} = 1.2539c^2$, $E_{N_p=39} = 1.3414c^2$, and $E_{N_p=47} = 1.4700c^2$, which locate the left side of Fig. 11(b). It

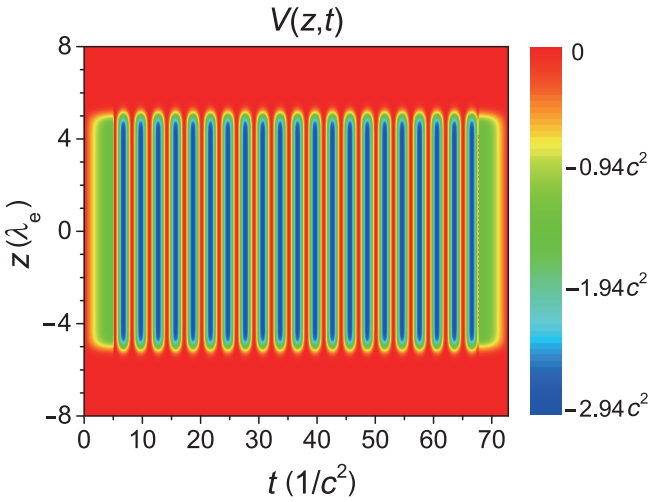

Fig. 10. Contour plot of the potential $V(z, t)$. The fields parameters are $V_1 = V_2 = 2c^2-10{,}000$, $\omega = 2.1c^2$, $D = 10\lambda_e$, and $W = 0.3\lambda_e$. Other parameters are $t_0 = 5/c^2$ and $t_1 = 20\pi/c^2$.

seems that they have a somewhat more complex relation. In fact by our studies in detail in Ref. [60], we conclude that these peaks come from the high-order effects in the interaction between the energy levels and the "photons" since $E_{N_p=9} = E_3 + E_4 + \omega - c^2$, $E_{N_p=33} = E_1 + E_2 + E_3 + \omega$, $E_{N_p=39} = E_1 + E_2 + \omega$, and $E_{N_p=47} = E_1 + E_2 + E_4 + \omega$. Also we found that $E_{N_p=150} = E_0 + 2\omega$ in Fig. 11(c) as well as $E_{N_p=242} = E_0 + 3\omega$ in Fig. 11(d) with $E_0 \approx E_1 + E_2 + E_4 = -0.64c^2$. This indicates that there exist some resonances among different levels assisted by multiphoton process for the pair production. Generally from Fig. 11(c) and (d), one can also get the relation of $E_{pn} = E_n + m\omega$ for each peaks of $n = 1,2,3,4,5,6,7,8$, where $m = 2$ or/and 3 denote two-photon and three-photon processes, respectively.

From the view point of CQFT, there exists a relation between the momentum of the created electrons and the eigenenergy of the bound states in the multiphoton pair creation process strongly. Evenly the pair production by multiphoton process can occur when the applied fields are subcritical in the sense of Schwinger critical field. On the other hand, obviously the multiphoton pair production can be got also via other different research approaches such as S-matrix, QVE and DHW mentioned before, which can be considered as some important complementary and comparable methods to the study by CQFT here.

7. Conclusion, discussion and outlook

In summary, in this review paper, we have presented many interesting results of e^+e^- pair production in ultrastrong laser fields, including the dependence of e^+e^- pair momentum distribution and number density on field parameters, by employing some important research approaches such as worldline instantons, S-matrix, QVE, DHW, and CQFT, etc.

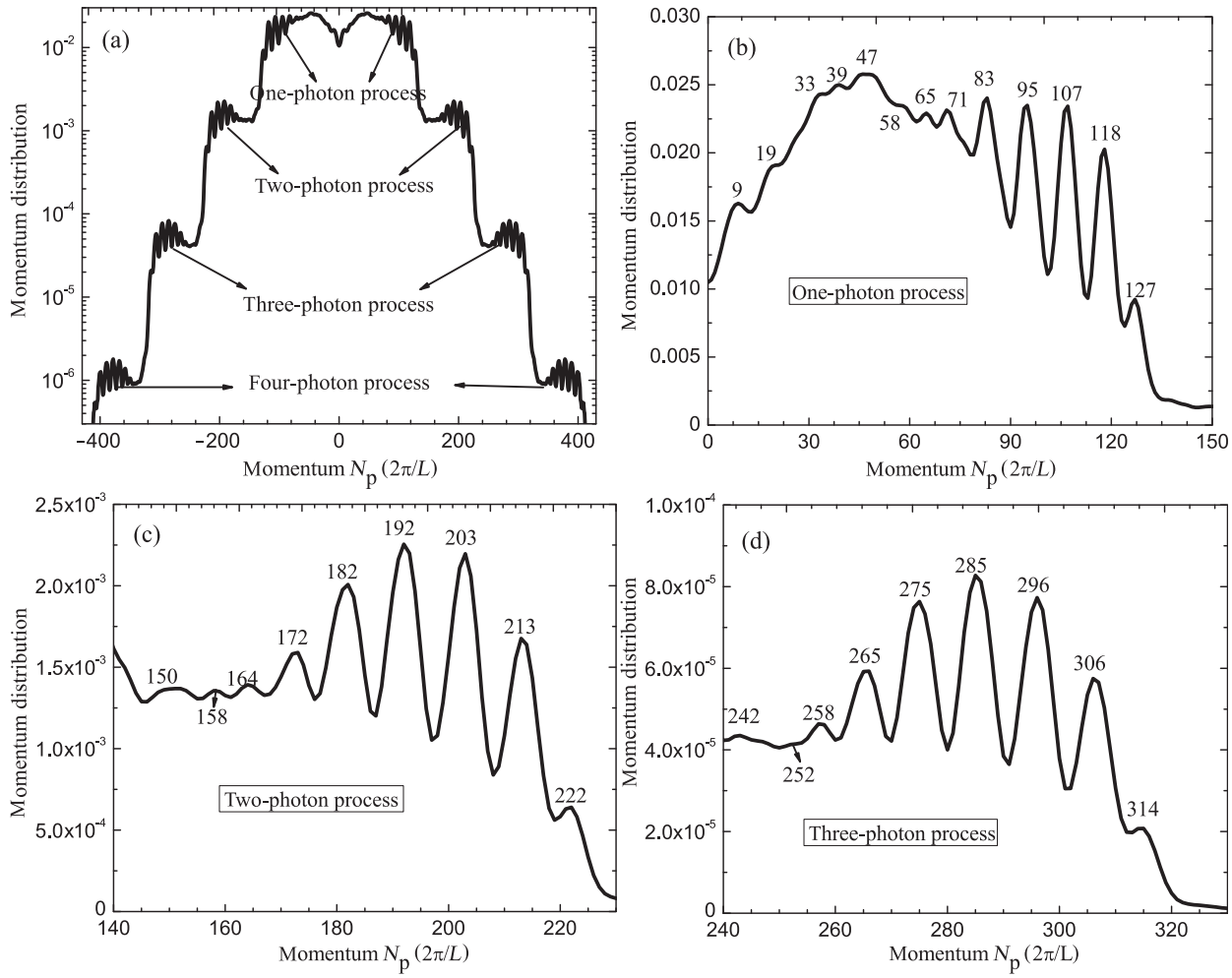

Fig. 11. Momentum distribution of the created particles for the combined fields. The fields parameters are $D = 10\lambda_e$, $W = 0.3\lambda_e$, $V_1 = V_2 = 2c^2-10{,}000$, $\omega = 2.1c^2$. Other parameters are $L = 2.0$, $N_z = 4096$, $t_0 = 5/c^2$, $t_1 = 20\pi/c^2$ and $T = 2t_0 + t_1 = (10+20\pi)/c^2$ and $N_t = 30{,}000$. This figure is from Ref. [60].

Table 1
The values of E_{pi} and E_i corresponding to the 8 peaks of $N_p = 58$, 65, 71, 83, 95, 107, 118, 127 in Fig. 11(b).

i	1	2	3	4	5	6	7	8
N_p	58	65	71	83	95	107	118	127
E_{pi}	$1.6637c^2$	$1.7946c^2$	$1.9299c^2$	$2.1496c^2$	$2.4174c^2$	$2.6490c^2$	$2.8841c^2$	$3.0785c^2$
E_i	$-0.4247c^2$	$-0.3069c^2$	$-0.1361c^2$	$0.0680c^2$	$0.2919c^2$	$0.5260c^2$	$0.7618c^2$	$0.9778c^2$

Particularly, our works are chosen to be immersed into the effects of electric field polarization on vacuum pair production numerically by employing different approaches like of worldline instantons, *S*-matrix and the real-time DHW formalism. It is found that the optimal pair production corresponds to an elliptic polarization in some cases. The effect of polarization on the momentum spectra of created particles is very delicated, for instance, for a multi-cycle field the momentum distribution can split into two segments in the transverse direction and then connect into a ring by increasing the polarization. This result is similar to the one in SFI. By studying the effect of polarization on the number density of created e^+e^- pairs, we find that for a small laser frequency, the particle number density deceases with polarization. However, for a large laser frequency, the number density can reach its maximum value at linear polarization, circular polarization, or even elliptical polarization, which seems to be counter-intuitive.

Due to the use of a general polarized field, our studies not only reveal several characteristics of pair production which can not be captured by a linearly polarized or circularly polarized field, such as the split of momentum spectrum, but also link up pair production with similar phenomena in SFI where some experiments are ongoing. Furthermore, because of the limitation in experiment instruments, a perfect circularly polarized field is harder to be produced than an elliptically

polarized one. So we believe that our studies about the elliptic polarization are also more closely associated with the experiment interests.

Besides the study aforementioned about the e^+e^- pair production, some other involved researches are also interesting. These fields include the muon pair production [104,105], the cascade e^+e^- pair production by laser interacting with electron beams [106,107], the e^+e^- pair production by laser irradiating plasmas [108], the properties of ultra-relativistic electron-positron plasmas [109], QED birefringence problem in a thermal relativistic pair plasma [110] and so on. However, they are not the main topic of this review paper.

Upon further research on e^+e^- pair production from vacuum in ultrastrong laser fields, we remind the reader to care about two aspects. One is the newest development of existing methods to the new field configurations or/and new problems. For example, Dumlu extended the worldline instantons research to the multi-dimensional quantum tunneling in the Schwinger effect [77]. He found that the worldlines were multiperiodic, and the periods of motion collectively depended on the strength of spatial and temporal inhomogeneity. More recently Schneider and Schützhold [111] studied the subleading prefactor in front of the exponential using the worldline instanton method and found that the main features of the dynamically assisted Sauter-Schwinger effect, including the dependence on the shape of the weaker field, were basically unaffected by the prefactor. Comparison of semiclassical and Wigner function methods for pair production in rotating fields can be seen in Ref. [112]. Using QVE research method, recently, we performed two works for the pair production in one- and two-color field with frequency chirping [113] and the modulation effect in multiphoton pair production [114]. A recent work with CQFT can refer to that [115] by Wang, Liu and Fu wherein as they showed that e^+e^- pairs could be pumped inexhaustibly with a constant production rate from the vacuum under a very strong well potential with oscillating width or depth. Moreover, a modified CQFT approach is developed to study the e^+e^- pair production in external electric fields varying both in space and time by Aleksandrov, Plunien and Shabaev [116]. The stochastic quantization now has also been used as another promising tool to investigate pair creation [117].

The other newest development aspect of the topic, maybe more important, is that the pair production study which has been extended to the particle-antiparticle production under fields different from U(1) gauge, for example, under non-Abelian SU(2) or/and SU(3) fields in the framework of quantum chromodynamics (QCD). Even the corresponding cases are studied in the string theory by a famous AdS-CFT correspondence principle, where AdS and CFT are the abbreviation of the Anti-de Sitter space and the conformal field theory, respectively. For QCD case, fermion pair production in non-Abelian gauge fields has a long tradition in the heavy ion community and many important works have been done [118,119]. Besides, many authors have made efforts to reveal the quark-antiquark production and the Casimir dependence of the transverse distribution in non-Abelian particle production [120–122]. Also of note is that the real-time lattice gauge theory and/or classical-statistical field theory approach which has been a powerful tool to study strong-field QED in space-time dependent electromagnetic fields is now used to study pair creation in the context of non-Abelian gauge field theories [123–126]. For the case involving of string theory, Semenoff and Zarembo [127] studied the tunneling pair creation of W bosons by an external electric field on the Coulomb branch of $N = 4$ supersymmetric Yang–Mills theory, where they used AdS/CFT holography to find a generalization of Schwinger formula for the pair production rate to the strong coupling, planar limit which includes the exchange of virtual massless particles to all orders. Sonner [128] showed that the recently proposed bulk dual of an entangled pair of quark-antiquark corresponded to the Lorentzian continuation of the tunneling instanton describing Schwinger pair creation in the dual field theory. By using AdS-CFT, in the work of Ref. [129], Ghodrati studied the critical electric field, the Schwinger pair creation rate and the potential phase diagram for the quark-antiquark production in the typical four confining supergravity backgrounds. It is found that the phase transitions have different rates in different supergravity backgrounds. Very recently we also tried to extend our research from QED to QCD case for the pair production in strong SU(2) background fields [130]. While the treatment is in classical framework, it is interesting to find that the momentum distribution of the particle is first centered on two islands but gradually split into narrower region on the color charge sphere. It ultimately reaches a steady state that is related to the field amplitude and variation. The problem is under active study by us now, and complete quantum treatment is needed to reveal the physics behind it.

Therefore the topic of present review tells us that pair production from vacuum in ultrastrong laser fields is still an open problem in both theoretical challenging feature as well as the experimental realization. It is a highly interdisciplinary field which will affect the deep understanding of basic QED, quantum vacuum, nonlinear science and the properties of early universe stage. The techniques contents behind the theoretical studies maybe have potential applications to many fields such as the detection of the features of applied external laser fields as well as the created particles.

Acknowledgements

Authors are grateful to Profs. S.G. Chen, L.B. Fu, J. Liu, B.F. Shen, Y.J. Li, S.B. Liu and Y.S Huang for helpful discussions on the pair production problem involving the topic of this review paper in the past years. This work was supported by the National Natural Science Foundation of China (NSFC) under Grant Nos. 11475026, 11175023 and also supported partially by the Open Fund of National Laboratory of Science and Technology on Computational Physics at IAPCM and the Fundamental Research Funds for the Central Universities (FRFCU). The computation was carried out at the High Performance Scientific Computing Center (HSCC) of the Beijing Normal University.

References

[1] P.A.M. Dirac, The quantum theory of the electron, Proc. Roy. Soc. Lond. A 117 (1928) 610−624.
[2] C.D. Anderson, The positive electron, Phys. Rev. 43 (1933), 491C494.
[3] F. Sauter, Ber das Verhalten eines Elektrons im homogenen elektrischen Feld nach der relativistischen Theorie Diracs, Z. Phys. 69 (1931) 742−764.
[4] W. Heisenberg, H. Euler, Consequences of Dirac's theory of positrons, Z. Phys. 98 (1936) 714−732.
[5] J. Schwinger, On gauge invariance and vacuum polarization, Phys. Rev. 82 (1951) 664−679.
[6] N.B. Narozhnyi, A.I. Nikishov, The simplest processes in the pair creating electric field, Yad. Fiz. 11 (1970) 1072 [Sov. J. Nucl. Phys. 11 (1970) 596].
[7] V.S. Popov, Pair production in a variable external field (quasiclassical approximation), Sov. Phys. JETP 34 (1972) 709.
[8] E. Brezin, C. Itzykson, Pair production in vacuum by an alternating field, Phys. Rev. D. 2 (1970) 1191−1199.
[9] T. Tajima, G. Mourou, Zettawatt-exawatt lasers and their applications in ultrastrong-field physics, Phys. Rev. ST Accel. Beams 5 (2002) 031301.
[10] G.A. Mourou, T. Tajima, S.V. Bulanov, Optics in the relativistic regime, Rev. Mod. Phys. 78 (2006) 309−371.
[11] V. Yanovsky, V. Chvykov, G. Kalinchenko, P. Rousseau, T. Planchon, et al., Ultra-high intensity- 300-TW laser at 0.1 Hz repetition rate, Opt. Express 16 (2008) 2109−2114.
[12] ELI: http://www.eli-beams.eu/.
[13] XCELS: http://www.xcels.iapras.ru/.
[14] HiPER: http://www.hiper-laser.org/.
[15] L.D. Landau, E.M. Lifshitz, The Classical Theory of Fields, Elsevier, Oxford, 1975.
[16] E.J. Moniz, D.H. Sharp, Radiation reaction in nonrelativistic quantum electrodynamics, Phys. Rev. D 15 (1977) 2850−2865.
[17] C. Harvey, T. Heinzl, M. Marklund, Symmetry breaking from radiation reaction in ultra-intense laser fields, Phys. Rev. D 84 (2011) 116005.
[18] C. Harvey, M. Marklund, Radiation damping in pulsed Gaussian beams, Phys. Rev. A 85 (2012) 013412.
[19] V.B. Berestetskii, E.M. Lifshitz, L.P. Pitaevskii, Quantum Electrodynamics, Elsevier Butterworth-Heinemann, Oxford, 1982.
[20] W. Dittrich, M. Reuter, Effective Lagrangians in Quantum Electrodynamics, Springer, Heidelberg, 1985.
[21] W. Dittrich, H. Gies, Probing the Quantum Vacuum, Springer, Heidelberg, 2000.
[22] A. Ringwald, Pair production from vacuum at the focus of an X-ray free electron laser, Phys. Lett. B 510 (2001) 107−116.
[23] http://www.xfel.eu/.
[24] R. Alkofer, M.B. Hecht, C.D. Roberts, S.M. Schmidt, D.V. Vinnik, Pair creation and an X-ray free electron laser, Phys. Rev. Lett. 87 (2001) 193902.
[25] C.D. Roberts, S.M. Schmidt, D.V. Vinnik, Quantum effects with an X-ray free-electron laser, Phys. Rev. Lett. 89 (2002) 153901.
[26] A. Di Piazza, C. Müller, K.Z. Hatsagortsyan, C.H. Keitel, Extremely high-intensity laser interactions with fundamental quantum systems, Rev. Mod. Phys. 84 (2012) 1177−1228.
[27] I.K. Affleck, O. Alvarez, N.S. Manton, Pair production at strong coupling in weak external fields, Nucl. Phys. B 197 (1982) 509−519.
[28] S.P. Kim, D.N. Page, Schwinger pair production via instantons in strong electric fields, Phys. Rev. D 65 (2002) 105002.
[29] G.V. Dunne, C. Schubert, Worldline instantons and pair production in inhomogenous fields, Phys. Rev. D 72 (2005) 105004.
[30] G.V. Dunne, Q.H. Wang, Multidimensional worldline instantons, Phys. Rev. D 74 (2006) 065015.
[31] R. Schützhold, H. Gies, G. Dunne, Dynamically assisted Schwinger mechanism, Phys. Rev. Lett. 101 (2008) 130404.
[32] B.S. Xie, M. Mohamedsedik, S. Dulat, Electron-positron pair production in an elliptic polarized time varying field, Chin. Phys. Lett. 29 (2012) 021102.
[33] C. Muller, A.B. Voitkiv, N. Grun, Differential rates for multiphoton pair production by an ultrarelativistic nucleus colliding with an intense laser beam, Phys. Rev. A 67 (2003) 063407.
[34] C. Müller, A.B. Voitkiv, N. Grün, Nonlinear bound-free pair creation in the strong electromagnetic fields of a heavy nucleus and an intense X-ray laser, Phys. Rev. Lett. 91 (2003) 223601.
[35] C. Deneke, C. Muller, Bound-free e^+e^- pair creation with a linearly polarized laser field and a nuclear field, Phys. Rev. A 78 (2008) 033431.
[36] H.Y. Hu, C. Müller, C.H. Keitel, Complete QED theory of multiphoton trident pair production in strong laser fields, Phys. Rev. Lett. 105 (2010) 080401.
[37] A. Ilderton, Trident pair production in strong laser pulses, Phys. Rev. Lett. 106 (2011) 020404.
[38] L.Y. He, B.S. Xie, X.H. Guo, H.Y. Wang, Electron-positron pair production in an arbitrary polarized ultrastrong laser field, Commun. Theor. Phys. 58 (2012) 863−871.
[39] S.S. Bulanov, Pair production by a circularly polarized electromagnetic wave in a plasma, Phys. Rev. E 69 (2004) 036408.
[40] C.K. Dumlu, G.V. Dunne, Stokes phenomenon and Schwinger vacuum pair production in time-dependent laser pulses, Phys. Rev. Lett. 104 (2010) 250402.
[41] E. Akkermans, G.V. Dunne, Ramsey fringes and time-domain multiple-slit interference from vacuum, Phys. Rev. Lett. 108 (2012) 030401.
[42] Z.L. Li, D. Lu, B.S. Xie, Multiple-slit interference effect in the time domain for boson pair production, Phys. Rev. D 89 (2014) 067701.
[43] E. Strobel, S.S. Xue, Semiclassical pair production rate for rotating electric fields, Phys. Rev. D 91 (2015) 045016.
[44] D.B. Blaschke, A.V. Prozorkevich, C.D. Roberts, S.M. Schmidt, S.A. Smolyansky, Pair production and optical lasers, Phys. Rev. Lett. 96 (2006) 140402.
[45] F. Hebenstreit, R. Alkofer, G.V. Dunne, H. Gies, Momentum signatures for Schwinger pair production in short laser pulses with a subcycle structure, Phys. Rev. Lett. 102 (2009) 150404.
[46] A. Nuriman, B.S. Xie, Z.L. Li, D. Sayipjamal, Enhanced electron-positron pair creation by dynamically assisted combinational fields, Phys. Lett. B 717 (2012) 465−469.
[47] N. Abdukerim, Z.L. Li, B.S. Xie, Effects of laser pulse shape and carrier envelope phase on pair production, Phys. Lett. B 726 (2013) 820−826.
[48] Z.L. Li, D. Lu, B.S. Xie, L.B. Fu, J. Liu, B.F. Shen, Enhanced pair production in strong fields by multiple-slit interference effect with dynamically assisted Schwinger mechanism, Phys. Rev. D 89 (2014) 093011.
[49] C. Kohlfürst, H. Gies, R. Alkofer, Effective mass signatures in multi-photon pair production, Phys. Rev. Lett. 112 (2014) 050402.
[50] A. Blinne, H. Gies, Pair production in rotating electric fields, Phys. Rev. D 89 (2014) 085001.
[51] Z.L. Li, D. Lu, B.S. Xie, Effects of electric field polarizations on pair production, Phys. Rev. D 92 (2015) 085001.
[52] Z.L. Li, D. Lu, B.S. Xie, B.F. Shen, L.B. Fu, J. Liu, Nonperturbative signatures in pair production for general elliptic polarization fields, Europhys. Lett. 110 (2015) 51001.
[53] J.W. Braun, Q. Su, R. Grobe, Numerical approach to solve the time-dependent Dirac equation, Phys. Rev. A 59 (1999) 604−612.
[54] P. Krekora, Q. Su, R. Grobe, Klein paradox in spatial and temporal resolution, Phys. Rev. Lett. 92 (2004) 040406.
[55] P. Krekora, Q. Su, R. Grobe, Relativistic electron localization and the lack of zitterbewegung, Phys. Rev. Lett. 93 (2004) 043004.
[56] P. Krekora, Q. Su, R. Grobe, Klein paradox with spin-resolved electrons and positrons, Phys. Rev. A 72 (2005) 064103.
[57] P. Krekora, K. Cooley, Q. Su, R. Grobe, Creation dynamics of bound states in supercritical fields, Phys. Rev. Lett. 95 (2005) 070403.
[58] C.C. Gerry, Q. Su, R. Grobe, Timing of pair production in time-dependent force fields, Phys. Rev. A 74 (2006) 044103.
[59] M. Jiang, W. Su, Z.Q. Lv, X. Lu, Y.J. Li, et al., Pair creation enhancement due to combined external fields, Phys. Rev. A 85 (2012) 033408.

[60] S. Tang, B.S. Xie, D. Lu, H.Y. Wang, L.B. Fu, J. Liu, Electron-positron pair creation and correlation between momentum and energy level in a symmetric potential well, Phys. Rev. A 88 (2013) 012106.
[61] F. Hebenstreit, J. Berges, D. Gelfand, Simulating fermion production in 1+1 dimensional QED, Phys. Rev. D 87 (2013) 105006.
[62] V. Kasper, F. Hebenstreit, J. Berges, Fermion production from real-time lattice gauge theory in the classical-statistical regime, Phys. Rev. D 90 (2014) 025016.
[63] N. Mueller, F. Hebenstreit, J. Berges, Anomaly-induced dynamical refringence in strong-field QED, Phys. Rev. Lett. 117 (2016) 061601.
[64] F. Gelis, N. Tanji, Formulation of the Schwinger mechanism in classical statistical field theory, Phys. Rev. D 87 (2013) 125035.
[65] D.L. Burke, R.C. Field, G. Horton-Smith, J.E. Spencer, D. Walz, et al., Positron production in multiphoton light-by-light scattering, Phys. Rev. Lett. 79 (1997) 1626−1629.
[66] C. Bamber, S.J. Boege, T. Koffas, T. Kotseroglou, A.C. Melissinos, et al., Studies of nonlinear QED in collisions of 46.6 GeV electrons with intense laser pulses, Phys. Rev. D 60 (1999) 092004.
[67] L.V. Keldysh, Ionization in the field of a strong electromagnetic wave, Sov. Phys. JETP 20 (1965) 1307−1314.
[68] A.M. Perelomov, V.S. Popov, M.V. Terentév, Ionization of atoms in an alternating electric field, Sov. Phys. JETP 23 (1966) 924−934.
[69] A.M. Perelomov, V.S. Popov, M.V. Terentév, Ionization of atoms in an alternating electric field: II, Sov. Phys. JETP 24 (1967) 207−217.
[70] V.I. Usachenko, V.A. Pazdzersky, J.K. McIver, Reexamination of high-energy above-threshold ionization (ATI): an alternative strong-field ATI model, Phys. Rev. A 69 (2004) 013406.
[71] Y.V. Vanne, A. Saenz, Exact Keldysh theory of strong-field ionization: residue method versus saddle point approximation, Phys. Rev. A 75 (2007) 033403.
[72] C. Bula, K.T. McDonald, E.J. Prebys, C. Bamber, S. Boege, et al., Observation of nonlinear effects in Compton scattering, Phys. Rev. Lett. 76 (1996) 3116−3119.
[73] J. Reinhardt, W. Greiner, Quantum electrodynamics of strong fields, Rept. Prog. Phys. 40 (1977) 219−295.
[74] R.P. Feynman, An operator calculus having applications in quantum electrodynamics, Phys. Rev. 84 (1951) 108−128.
[75] C. Schubert, Perturbative quantum field theory in the string-inspired formalism, Phys. Rep. 355 (2001) 73−234.
[76] V.S. Popov, M.S. Marinov, E^+E^- pair production in variable electric field, Yad. Fiz. 16 (1972) 809 [Sov. J. Nucl. Phys. 16 (1973) 449].
[77] C.K. Dumlu, Multidimensional quantum tunneling in the Schwinger effect, Phys. Rev. D 93 (2016) 065045.
[78] D.M. Volkov, Über eine Klasse von Lösungen der Diracschen Gleichung, Z. Phys. 94 (1935) 250−260.
[79] H.R. Reiss, Absorption of light by light, J. Math. Phys. 3 (1962) 59−67.
[80] A.I. Nikishov, V.I. Ritus, Quantum processes in the field of a circularly polarized electromagnetic wave, Sov. Phys. JETP 19 (1964) 769−796.
[81] W. Greiner, J. Reinhardt, Quantum Electrodynamics, fourth ed., Springer-Verlag, Berlin Heidelberg, 2009.
[82] M. Mohamedsedik, B.S. Xie, S. Dulat, Analytical study of pair production rate from vacuum in an elliptic polarized field by a two-level transition technique, Commun. Theor. Phys. 57 (2012) 422.
[83] S. Schmidt, D. Blaschke, G. Röpke, S.A. Smolyansky, A.V. Prozorkevich, et al., A quantum kinetic equation for particle production in the Schwinger mechanism, Int. J. Mod. Phys. E 7 (1998) 709.
[84] S. Schmidt, D. Blaschke, G. Röpke, A.V. Prozorkevich, S.A. Smolyansky, et al., Non-markovian effects in strong-field pair creation, Phys. Rev. D 59 (1999) 094005.
[85] J.C.R. Bloch, V.A. Mizerny, A.V. Prozorkevich, C.D. Roberts, S.M. Schmidt, et al., Pair creation: back reactions and damping, Phys. Rev. D 60 (1999) 116011.
[86] F. Hebenstreit, F. Fillion-Gourdeau, Optimization of Schwinger pair production in colliding laser pulses, Phys. Lett. B 739 (2014) 189.
[87] M. Pont, M. Gavrila, Stabilization of atomic hydrogen in superintense, high-frequency laser fields of circular polarization, Phys. Rev. Lett. 65 (1990) 2362−2365.
[88] B.S. Xie, Classical intense-field stabilization analysis by four-dimensional mapapproximation, Phys. Lett. A 242 (1998) 79−82.
[89] C. Kohlfürst, Electron-positron pair production in structured pulses of electric fields, arXiv:1212.0880.
[90] C. Kohlfürst, M. Mitter, G. Von Winckel, F. Hebenstreit, R. Alkofer, Optimizing the pulse shape for Schwinger pair production, Phys. Rev. D 88 (2013) 045028.
[91] I. Bialynicki-Birula, P. Górnicki, J. Rafelski, Phase-space structure of the Dirac vacuum, Phys. Rev. D 44 (1991) 1825−1835.
[92] F. Hebenstreit, R. Alkofer, H. Gies, Schwinger pair production in space- and time-dependent electric fields: relating the Wigner formalism to quantum kinetic theory, Phys. Rev. D 82 (2010) 105026.
[93] F. Hebenstreit, R. Alkofer, H. Gies, Particle self-bunching in the Schwinger effect in spacetime-dependent electric fields, Phys. Rev. Lett. 107 (2011) 180403.
[94] C. Kohlfürst, R. Alkofer, On the effect of time-dependent inhomogeneous magnetic fields in electron−positron pair production, Phys. Lett. B 756 (2016) 371.
[95] G.R. Mocken, M. Ruf, C. Müller, C.H. Keitel, Nonperturbative multiphoton electron-positron−pair creation in laser fields, Phys. Rev. A 81 (2010) 022122.
[96] M. Ruf, G.R. Mocken, C. Müller, K.Z. Hatsagortsyan, C.H. Keitel, Pair production in laser fields oscillating in space and time, Phys. Rev. Lett. 102 (2009) 080402.
[97] C.K. Dumlu, G.V. Dunne, Interference effects in Schwinger vacuum pair production for time-dependent laser pulses, Phys. Rev. D. 83 (2011) 065028.
[98] A.N. Pfeiffer, C. Cirelli, M. Smolarski, D. Dimitrovski, M. Abu-samha, et al., Attoclock reveals natural coordinates of the laser-induced tunnelling current flow in atoms, Nat. Phys. 8 (2012) 76−80.
[99] A.N. Pfeiffer, C. Cirelli, A.S. Landsman, M. Smolarski, D. Dimitrovski, et al., Probing the longitudinal momentum spread of the electron wave packet at the tunnel exit, Phys. Rev. Lett. 109 (2012) 083002.
[100] C. Hofmann, A.S. Landsman, A. Zielinski, C. Cirelli, T. Zimmermann, et al., Interpreting electron-momentum distributions and nonadiabaticity in strong-field ionization, Phys. Rev. A 90 (2014) 043406.
[101] S.S. Schweber, An Introduction to Relativistic Quantum Field Theory, Harper & Row, New York, 1962.
[102] W. Greiner, Relativistic Quantum Mechanics: Wave Equations, third ed., Springer-Verlag, Berlin Heidelberg, 2000.
[104] C. Müller, K.Z. Hatsagortsyan, C.H. Keitel, Muon pair creation from positronium in a linearly polarized laser field, Phys. Rev. A 78 (2008) 033408.
[105] C. Müller, C. Deneke, C.H. Keitel, Muon-pair creation by two X-ray laser photons in the field of an atomic nucleus, Phys. Rev. Lett. 101 (2008) 060402.
[106] I.V. Sokolov, N.M. Naumova, J.A. Nees, G.A. Mourou, Pair creation in QED-strong pulsed laser fields interacting with electron beams, Phys. Rev. Lett. 105 (2010) 195005.
[107] S. Tang, M. Ali Bake, H.Y. Wang, B.S. Xie, QED cascades induced by high energy γ photon in strong laser field, Phys. Rev. A 89 (2014) 022105.
[108] C.P. Ridgers, C.S. Brady, R. Duclous, J.G. Kirk, K. Bennett, et al., Dense electron-positron plasmas and ultraintense rays from laser-irradiated solids, Phys. Rev. Lett. 108 (2012) 165006.
[109] M.H. Thoma, Colloquium: field theoretic description of ultrarelativistic electron-positron plasmas, Rev. Mod. Phys. 81 (2009) 959−968.
[110] Y.S. Huang, Quantum-electrodynamical birefringence vanishing in a thermal relativistic pair plasma, Sci. Rep. 5 (2015) 15866.
[111] C. Schneider, R. Schützhold, Prefactor in the dynamically assisted Sauter-Schwinger effect, Phys. Rev. D 94 (2016) 085015.
[112] A. Blinne, E. Strobel, Comparison of semiclassical and Wigner function methods in pair production in rotating fields, Phys. Rev. D 93 (2016) 025014.
[113] N. Abdukerim, Z.L. Li, B.S. Xie, Enhanced electron−positron pair production by frequency chirping in one- and two-color laser pulse fields, Chin. Phys. B 26 (2017) 020301.
[114] I. Sitiwaldi, B.S. Xie, Modulation effect in multiphoton pair production, Phys. Lett. B 768 (2017) 174−179.

[115] Q. Wang, J. Liu, L.B. Fu, Pumping electron-positron pairs from a well potential, Sci. Rep. 6 (2016) 25292.
[116] I.A. Aleksandrov, G. Plunien, V.M. Shabaev, Electron-positron pair production in external electric fields varying both in space and time, Phys. Rev. D 94 (2016) 065024.
[117] K. Fukushima, T. Hayata, Schwinger mechanism with stochastic quantization, Phys. Lett. B 735 (2014) 371.
[118] F. Gelis, K. Kajantie, T. Lappi, Chemical thermalization in relativistic heavy ion collisions, Phys. Rev. Lett. 96 (2006) 032304.
[119] P.M. Saffin, A. Tranberg, Real-time fermions for baryogenesis simulations, J. High Energy Phys. 7 (2011) 66.
[120] V.V. Skokov, P. Lvai, Transverse and longitudinal momentum spectra of fermions produced in strong SU(2) fields, Phys. Rev. D. 78 (2008) 054004.
[121] F. Cooper, J.F. Dawson, B. Mihaila, Casimir dependence of transverse distribution of pairs produced from a strong constant chromoelectric background field, Phys. Rev. D 78 (2008) 117901.
[122] J.F. Dawson, B. Mihaila, F. Cooper, Dynamics of particle production by strong electric fields in non-Abelian plasmas, Phys. Rev. D 81 (2010) 054026.
[123] D. Gelfand, F. Hebenstreit, J. Berges, Early quark production and approach to chemical equilibrium, Phys. Rev. D 93 (2016) 085001.
[124] P.V. Buividovich, M.V. Ulybyshev, Numerical study of chiral plasma instability within the classical statistical field theory approach, Phys. Rev. D 94 (2016) 025009.
[125] N. Müller, S. Schlichting, S. Sharma, Chiral magnetic effect and anomalous transport from real-time lattice simulations, Phys. Rev. Lett. 117 (2016) 142301.
[126] F. Gelis, N. Tanji, Quark production in heavy ion collisions: formalism and boost invariant fermionic light-cone mode functions, J. High Energy Phys. 2 (2016) 126.
[127] Gordon W. Semenoff, Konstantin Zarembo, Holographic schwinger effect, Phys. Rev. Lett. 107 (2011) 171601.
[128] J. Sonner, Holographic Schwinger effect and the geometry of entanglement, Phys. Rev. Lett. 111 (2013) 211603.
[129] M. Ghodrati, Schwinger effect and entanglement entropy in confining geometries, Phys. Rev. D 92 (2016) 065015.
[130] M.R. Jia, Z.L. Li, C. Lv, F. Wan, B.S. Xie, Pair production in strong SU(2) background fields, Front. Phys. 12 (2017) 121101.